

A State Augmented Adaptive Backstepping Control of Wheeled Mobile Robots

Seyed Mohammad Ahmadi*, Mojtaba Behnam Taghadosi, AmirReza Haqshenas M.
Department of Electrical Engineering, Imam Reza International University
9138833186, Mashhad, Iran

*Corresponding Author: s.m.ahmadi1365@gmail.com; ahmadi@imamreza.ac.ir

Abstract. The present paper aims to design an integrated kinematic/dynamic-based tracking controller for wheeled mobile robots considering motors' dynamics. By defining a reference wheeled mobile robot, the role of kinematic controller is to not only minimize the posture error which indicates the difference between the reference and actual wheeled mobile robots, but also to generate a desired path for the actual wheeled mobile robot. The kinematic tracking control problem of wheeled mobile robots is so challenging if motors' dynamics, parametric and nonparametric uncertainties and external disturbances are considered. Thus, proposing a dynamic control law alongside a kinematic control is unavoidable. In this study, we propose a new dynamic controller namely, a state augmented adaptive backstepping such that the desired path is asymptotically tracked. Several numerical results accompanied by 3D simulations of trajectory tracking control of a wheeled mobile robot in "Simscape Multibody" environment and comparisons with two well-designed controllers in the literature are reported to show the high-performance of proposed control structure.

Keywords: Wheeled mobile robot; Backstepping; Adaptive Taylor series; State augmented; Simscape Multibody.

1. Introduction

One cannot doubt the fact that robotic systems are acting an increasingly key role in modern industries. Advanced facilities have been tending to use robots with the ability of movement in order to yield better and faster results in various tasks. As a result, taking the advantages of wheels and the robot's simple platform, wheeled mobile robots (WMRs) provide the most common means of mobility and therefore become a trend category in mobile robots (Klančar et al., 2017). Having different configurations for WMRs, there are two major types of wheels, namely active wheels which are connected to chassis through motors and castor(s) which can be connected directly to chassis (Delgado-Mata et al., 2012). Among many driving techniques, differential drive wheeled mobile robots (Klančar et al., 2017) keep the attention of many researchers since producing different rotational velocities between two motors attached to active wheels is one of the simplest ways to drive WMRs. Thus, designing an efficient controller for these types of robotic systems has been put into the spotlight for control researchers.

In order to track a desired path, some literature has tended to control the linear and angular velocities of differential drive WMRs through its kinematics. Kanayama et al. (1988) proposed a kinematic control law via dead-reckoning for posture update along with the Proportional-Integral-Derivative (PID) structure. Afterwards, introducing differential equations for errors in position and orientation of WMR, a kinematic controller (Kanayama et al., 1990) has been designed based on backstepping and feedforward control toolboxes. The time-varying state feedback alongside back-stepping technique was taken to work to design a kinematic controller (JIANGdagger and Nijmeijer, 1997) for WMRs. Considering the kinematics of unicycle as a reference and proving the controllability of Cartesian motion equations of unicycle, De Luca et al. (2001) developed a chained form kinematic equation for WMRs and introduced a nonlinear time-varying kinematic controller. Using a generic modeling and online computational methods, Bayle et al. (2002) designed a kinematic controller for a mobile manipulator. In order to propose a kinematic control for a differentially driven mobile manipulator containing steering wheels, an input-output linearization control method (De Luca et al., 2010) has been used. Utilizing feedforward inputs along with state feedback and the flatness property of system, a kinematic controller (Klančar et al., 2011) has been proposed for a group of WMRs. To minimize the designed quadratic function which is a function of tracking errors and control effort, a model-predictive trajectory control (Škrjanc and Klančar, 2017) and a nonlinear model

predictive control (Nascimento et al., 2018) for WMRs have been developed. A kinematic-based output feedback control law (Wu et al., 2018) has been designed for the finite-time trajectory tracking control of WMR.

In practice, WMRs are often exposed to high-speed operations, changing lane maneuvers and carrying loads which lead to parametric and non-parametric uncertainties. Therefore, control methods are needed to be designed with more accuracy in the presence of uncertainties as well as to have faster responses. A key problem with much of the literature in relation to kinematic-based controllers is that they have neglected the dynamics of WMRs and their effects on the procedure of control design. For that reason, dynamic control laws have been raising up to bring about more accuracy than lone kinematic controllers. A sliding mode toolbox was utilized to propose a torque-based dynamic tracking control scheme (Yang and Kim, 1999) in polar space for WMRs. To tackle parametric and non-parametric uncertainties, a torque-based robust adaptive control law (Dong et al., 2005), a voltage-based adaptive feedback linearizing controller (Shojaei et al., 2011) and an indirect adaptive Taylor series controller (Haqshenas M. et al., 2019) have been developed. By defining a two-dimensional output vector to decouple robot's two control signals and using the backstepping methodology, Rudra et al. (2016) proposed a dynamic controller for WMRs. In order to design a robust dynamic impedance controller, Souzanchi-K et al. (2017) divided the WMR's model into two parts namely, a known nominal model and unknown dynamics. To compensate for un-modeled dynamics and modelling imperfection, the adaptive switching gain-based torque control (Roy, S. et al., 2017) has been designed as a dynamic controller.

Although dynamic control laws have brought the benefit of high accuracy to tracking problem of WMRs, there is a serious concern about these types of controllers. The majority of dynamic controllers are failed to compensate for the far initial conditions from a defined desired path. To address this concern, proposing an integrated kinematic/dynamic controller is inevitable. Via the strategy of torque control, a robust adaptive neural network control scheme (Fierro and Lewis, 1997), an adaptive backstepping control (Fukao et al., 2000), uncalibrated camera system-based adaptive tracking control (Dixon et al., 2001), a sliding mode control along with RFID sensor space (Lee et al., 2009), an adaptive state feedback controller utilizing two high-gain observers (Huang et al., 2014), an adaptive tracking control law without longitudinal velocity measurement (Shu et al., 2018), an adaptive variable control structure (Yang et al., 2018) and a nonsingular adaptive terminal sliding mode control (Zhai and Song, 2019) have been developed to design a kinematic/dynamic tracking controller for WMRs.

Considering the simplified dynamics of motors and defining a virtual control law, a simple adaptive kinematic/dynamic control law (Park et al., 2009) has been designed. By taking the advantages of backstepping toolbox and the sliding mode structure as the base for designing kinematic and dynamic control laws, respectively, Yue et al. (2013) proposed a robust scheme for the path following problem of WMR. Applying the recursive Gibbs–Appell method to derive the dynamical model of WMR, a torque-based tracking controller (Mirzaeinejad and Shafei, 2018) has been designed using a quadratic pointwise performance index. An input saturation technique and neural networks were gotten to work to develop a torque-based kinematic/dynamic robust tracking control (Huang et al., 2019) for WMRs. A kinematic/dynamic controller (Liu et al., 2020) utilizing an adaptive sliding mode approach for the online estimation of lumped disturbance applied to WMRs has been proposed.

Through the use of adaptive controllers, researchers are able to design suitable control laws for nonlinear systems which have unknown slowly time-varying parameters. The basic idea of adaptive schemes is to design adaptive rules to compensate for parametric uncertainties of a system (Slotine and Li, 1991). The most important limitation of an adaptive controller lies in the fact that this type of design has a poor performance when it comes to non-parametric uncertainties and external disturbances for nonlinear systems. Therefore, robust controllers come to light accompanying by adaptive designs to solve this problem (Ioannou and Sun, 1996). Generally, one can categorize adaptive controllers into two forms namely, direct and indirect adaptive control designs (Spooner et al., 2004). In a direct adaptive design, adaptive mechanisms act as control laws to tackle uncertainties. For example, a direct adaptive fuzzy-neural controller (Wang et al., 2002) and a direct adaptive control utilizing self-recurrent wavelet neural networks (Yoo et al., 2005, June) were developed to stabilize an inverted pendulum system and to control of a mobile robot, respectively. As another option, indirect adaptive controllers are developed such that uncertain nonlinear functions can be approximated in the structure of a control law by classical type of adaptive design or by universal approximation methods such as fuzzy systems, neural networks, or Taylor series polynomials. For example, by coupling the estimation of online parameters to sliding mode control structure, the tracking performance of a second order nonlinear system was improved (Slotine and Coetsee, 1986). For the tracking problem of a two degree of freedom semi-direct drive manipulator, an indirect adaptive control law was proposed (Slotine and Weiping, 1988). A robust adaptive control scheme (Le-Tien and Albu-Schäffer, 2017) based on a state feedback control method was designed for flexible-joint robots. A robust adaptive impedance scheme

along with a sliding mode observer (Azimi et al., 2018) and a model-based adaptive control (Azimi et al., 2019) were applied successfully to control lower-limb prostheses. Designing two inner and outer control loops, indirect adaptive Taylor series controllers (Haqshenas M. et al., 2020) were proposed for electrically-driven wheeled mobile robots.

Backstepping control is among the well-known investigated types of nonlinear control toolboxes on account of the recursive feedback control law and the Lyapunov stability theorem providing chattering-free control signals. The procedure of backstepping design is to recursively choose the appropriate functions of state variables namely, virtual control inputs for subsystems with fewer dimensions compared with the whole system in such a way that the Lyapunov function of nonlinear systems as well as actual control laws can be obtained (Kokotovic, 1992). The first study of backstepping is hard to trace in the literature. However, as it was mentioned in (Kokotovic, 1992), the backstepping structure was indirectly appeared in the work of (Tsinias, 1989; Byrnes et al., 1989 and Saberi et al., 1990), and since then Khalil (1992) introduced backstepping as a nonlinear control toolbox. Despite this interest, the issue regarding the classical structure of backstepping method is the explosion of complexity (Swaroop et al., 1997, June; Yip and Hedrick, 1998) especially for high-order nonlinear systems. To deal with this problem, Swaroop et al. (1997) proposed the Dynamic Surface Control (DSC) methodology for n -th order nonlinear systems and then Yip and Hedrick (1998) extended this technique to adaptive DSC compensating for uncertainties associated with a third-order system. In order to tackle parametric and non-parametric uncertainties, adaptive backstepping controllers have been gained much attention. However, these types of controllers may lead to overparameterization (Krstic et al. 1995). To address this problem, Krstic et al. (1995) suggested that adaptive rules can be treated as tuning functions in virtual control laws. Two modified adaptive backstepping control laws (Zhang et al. 2000) were studied for nonlinear systems containing an unknown high-frequency gain to alleviate the assumption on the sign of high-frequency gain via Nussbaum gains. Utilizing Nussbaum disturbance observer, an adaptive tracking dynamic surface backstepping control was designed for high-order strict-feedback nonlinear systems (Aghababa and Moradi, 2020). Adaptive fuzzy controllers along with the backstepping design (Shaocheng et al. 2009; Xin et al. 2020) were developed to control the process of two continuous stirred tank reactors. An adaptive backstepping nonsingular fast terminal sliding mode control (Van et al. 2018) was proposed for the tracking control of robotic manipulators. To avoid the explosion of complexity and overparameterization, an improved backstepping design (Bu, 2018; Bu, et al. 2018) was utilized for the tracking control of air-

breathing hypersonic vehicles (AHVs). In (Bu, 2018; Bu, et al. 2018), instead of using virtual control inputs in the classical structure of backstepping, intermediate variables were defined to design two separate control structure for the altitude and velocity tracking problems of AHVs. Benefited by using radial-basis-function neural networks and the funnel control scheme, uncertainties were compensated for the non-affine dynamics of AHVs and the semi-globally uniformly ultimately boundedness of states was guaranteed via the provided stability analysis. With the purpose of tracking control of wheeled mobile robots, the combination of adaptive DSC and virtual structure concept (Yoo et al. 2010), an adaptive DSC using radial-basis-function neural networks along with a nonlinear disturbance observer (Luo et al. 2014) and a backstepping fuzzy sliding mode control law (Wu et al. 2019) were designed.

To effectively compensate for the dynamics of motors, parametric and nonparametric uncertainties and dynamic external disturbances, this paper designs a new integrated kinematic/dynamic structure using an adaptive state augmented backstepping controller for the trajectory tracking of electrically-driven differential drive WMRs. Considering relatively far initial postures of the wheeled mobile robot compared with the reference path, the performance of designed controller is evaluated by several simulations. In addition, 3D simulations are also performed using “Simscape™ Multibody” environment of “MATLAB®” to show the better evaluation of tracking performance. For additional assessments, the proposed controller is analyzed and compared with two well-designed controllers (Roy, S. et al., 2017; Liu, K. et al., 2020). Let us represent the main contributions of this paper as follows:

- Ensuring the asymptotic convergence of tracking error and its time derivative, this paper presents a model-free controller using a new integrated kinematic/dynamic structure for differential drive WMRs by considering motors' dynamics.
- To the best of authors' knowledge, this is the first time of using a simple adaptive Taylor series approximator in the backstepping structure to design an efficient dynamic control law to avoid overparameterization.
- To obtain the high-performance in comparison with dynamic and integrated kinematic/dynamic controllers for WMRs, an additional state as an integral of the tracking error is added to the backstepping structure to form a state augmented backstepping control by a newly created subsystem.

- The proposed controller can compensate for parametric, non-parametric and time-varying external disturbances associated with electrically-driven differential drive WMRs.
- In addition to several simulations, detailed comparisons with two well-designed controllers are provided to show the efficiency of the proposed controller.

The rest of this scientific paper is organized as follows: *Section 2* formulates the kinematic control design. *Section 3* presents the integrated dynamics of electrically-driven wheeled mobile robot along with an adaptive state augmented backstepping dynamic controller and the analysis of Lyapunov-like closed-loop stability. In *Section 4*, numerous simulation results will be discussed. Finally, some concluding remarks are given in *Section 5*.

2. Problem Statement and Kinematic Controller Design

Figure. 1 illustrates a differential drive wheeled mobile robot formed from two front mounted castor wheels and two rear mounted active wheels actuated by two independent permanent magnet DC motors. The reference coordinate system, XOY, is used to determine the robot's position by $\mathbf{q} = [x \quad y \quad \theta]^T \in \mathbb{R}^{3 \times 1}$, in which θ is the counterclockwise orientation angle of mobile robot from X-axis and also x and y indicate the coordinates of point O_p . Moreover, $2b$ is the length between two active wheels, r_w is the radius of each active wheel, C is the mass center of mobile robot and d is the length between two points, namely C and O_p . The relation between the linear and angular velocities of each wheel can be formulated by

$$\dot{\phi}_{Ls} = \frac{v_{Ls}}{r_w} \quad (1)$$

$$\dot{\phi}_{Rs} = \frac{v_{Rs}}{r_w} \quad (2)$$

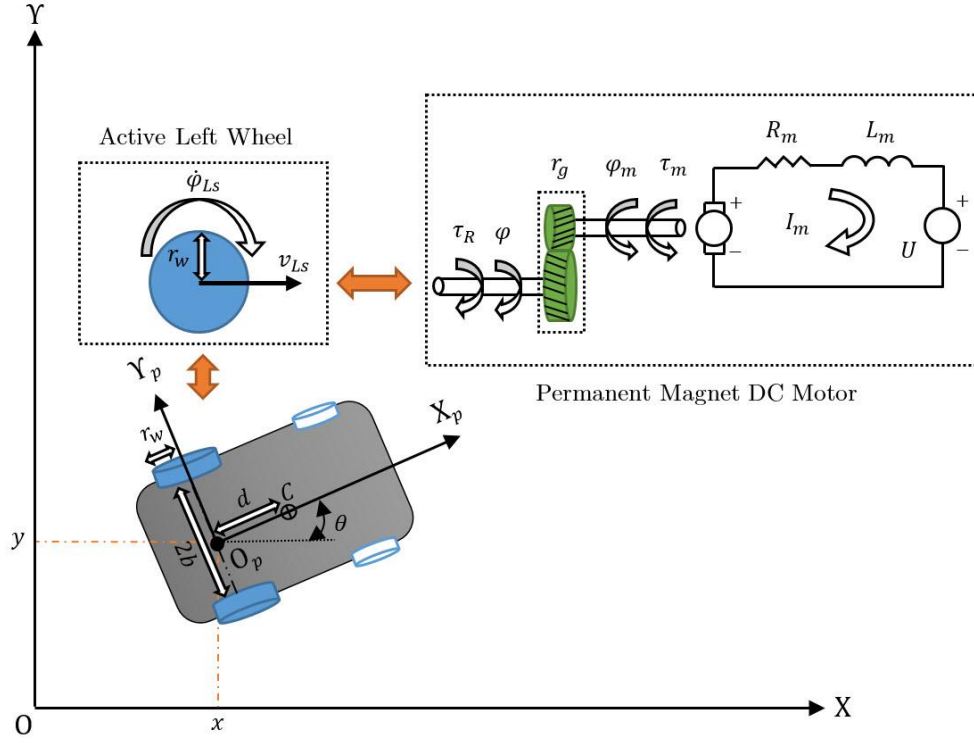


Figure. 1. An electrically-driven differential drive wheeled mobile robot.

where v_{LS} and $\dot{\phi}_{LS}$ represent the linear and angular velocities for the left wheel, respectively and v_{RS} and $\dot{\phi}_{RS}$ represent the linear and angular velocities for the right wheel, respectively. One can obtain the linear (v_l) and angular (ω) velocities of the mass center of a mobile robot via forward kinematics as follows

$$v_l = \frac{v_{RS} + v_{LS}}{2} \quad (3)$$

$$\omega = \frac{v_{RS} - v_{LS}}{2b} \quad (4)$$

By breaking v_l and ω into their components on X and Y axes, we have

$$\dot{x} = v_l \cos(\theta) \quad (5)$$

$$\dot{y} = v_l \sin(\theta) \quad (6)$$

$$\dot{\theta} = \omega \quad (7)$$

Let us rewrite equations (5-7) as follows

$$\dot{\mathbf{q}} = \mathbf{S}(\theta)\dot{\mathbf{h}} \quad (8)$$

where $\dot{\mathbf{h}} = [v_l, \omega]^T \in \mathbb{R}^{2 \times 1}$ represents the vector of linear and angular velocities of the mass center of a mobile robot, and the matrix $\mathbf{S}(\theta) \in \mathbb{R}^{3 \times 2}$ is given as

$$\mathbf{S}(\theta) = \begin{bmatrix} \cos \theta & 0 \\ \sin \theta & 0 \\ 0 & 1 \end{bmatrix} \quad (9)$$

To generate a desired path for an actual mobile robot, one can formulate the kinematics of reference wheeled mobile robot as follows (Kanayama et al., 1990)

$$\dot{\mathbf{q}}_{ref} = \mathbf{S}_{ref}(\theta)\dot{\mathbf{h}}_{ref} \quad (10)$$

where the vector $\dot{\mathbf{q}}_{ref} = [\dot{x}_{ref} \ \dot{y}_{ref} \ \dot{\theta}_{ref}]^T \in \mathbb{R}^{3 \times 1}$ denotes the reference linear velocities of wheeled mobile robot along X-axis (\dot{x}_{ref}) and Y-axis (\dot{y}_{ref}), and the reference angular velocity ($\dot{\theta}_{ref}$). The bounded vector $\dot{\mathbf{h}}_{ref}$ is represented as

$$\dot{\mathbf{h}}_{ref} = [v_{l_ref}, \omega_{ref}]^T \in \mathbb{R}^{2 \times 1} \quad (11)$$

where v_{l_ref} is the reference linear velocity, and ω_{ref} is the reference angular velocity. Also, via equation (9), the matrix $\mathbf{S}(\theta_{ref}) \in \mathbb{R}^{3 \times 2}$ is defined as

$$\mathbf{S}(\theta_{ref}) \triangleq \begin{bmatrix} \cos \theta_{ref} & 0 \\ \sin \theta_{ref} & 0 \\ 0 & 1 \end{bmatrix} \quad (12)$$

With the aim of designing a kinematic controller, the velocity control law is proposed to guarantee the asymptotic convergence of \mathbf{q} to \mathbf{q}_{ref} . To satisfy this demand, we define errors between the reference and real postures as follows

$$\boldsymbol{\epsilon} \triangleq \mathbf{q}_{ref} - \mathbf{q} = \begin{bmatrix} x_{ref} - x \\ y_{ref} - y \\ \theta_{ref} - \theta \end{bmatrix} \quad (13)$$

As illustrated in Figure. 2, the posture tracking error which denotes a transformation of \mathbf{q}_{ref} relative to the real mobile robot's fixed frame, i.e. e_{p1} , e_{p2} and e_{p3} , can be formulated by

$$e_{p1} = (x_{ref} - x)\cos\theta + (y_{ref} - y)\sin\theta \quad (14)$$

$$e_{p2} = -(x_{ref} - x)\sin\theta + (y_{ref} - y)\cos\theta \quad (15)$$

$$e_{p3} = \theta_{ref} - \theta \quad (16)$$

In other words, one can rewrite equations (13-16) as

$$\mathfrak{E}_p \triangleq \begin{bmatrix} e_{p1} \\ e_{p2} \\ e_{p3} \end{bmatrix} = \begin{bmatrix} \cos\theta & \sin\theta & 0 \\ -\sin\theta & \cos\theta & 0 \\ 0 & 0 & 1 \end{bmatrix} \mathfrak{E} \quad (17)$$

Using equations (8) and (10), the derivative of (17) with respect to time can be obtained as

$$\dot{e}_{p1} = -v_c + \omega_c e_{p2} + v_{l_ref} \cos e_{p3} \quad (18)$$

$$\dot{e}_{p2} = -\omega_c e_{p1} + v_{l_ref} \sin e_{p3} \quad (19)$$

$$\dot{e}_{p3} = -\omega_c + \omega_{ref} \quad (20)$$

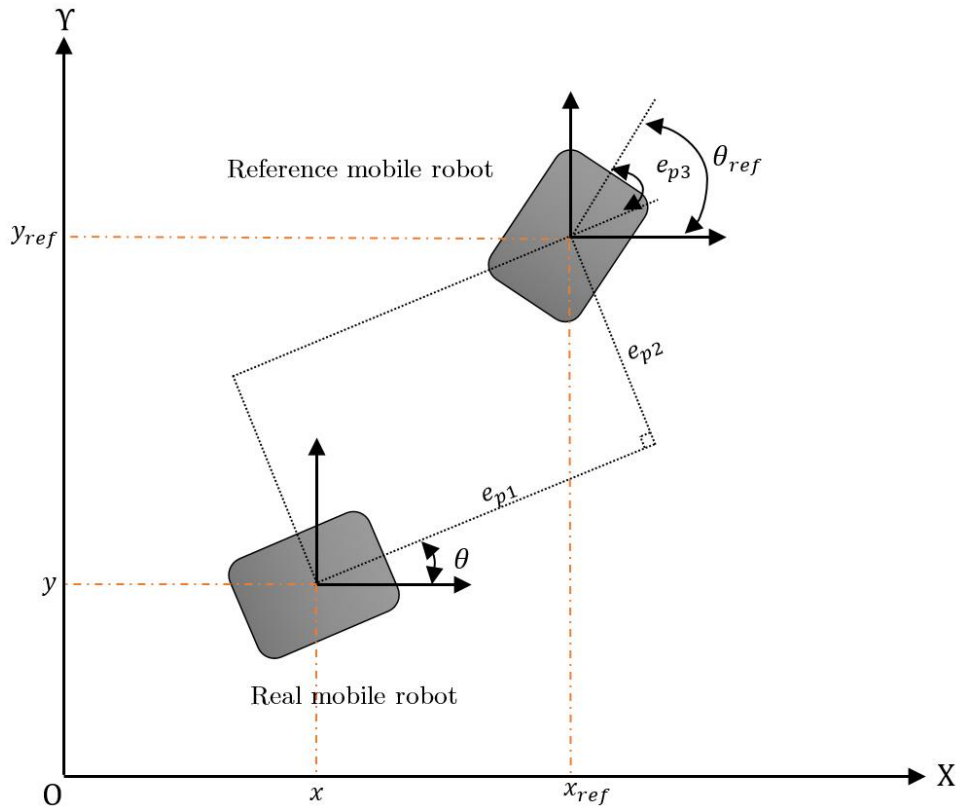


Figure. 2. Illustration of posture tracking error

In other words,

$$\dot{\mathfrak{E}}_p = \begin{bmatrix} \dot{e}_{p1} \\ \dot{e}_{p2} \\ \dot{e}_{p3} \end{bmatrix} = v_c \begin{bmatrix} -1 \\ 0 \\ 0 \end{bmatrix} + \omega_c \begin{bmatrix} e_{p2} \\ -e_{p1} \\ -1 \end{bmatrix} + \begin{bmatrix} v_{l_ref} \cos e_{p3} \\ v_{l_ref} \sin e_{p3} \\ \omega_{ref} \end{bmatrix} \quad (21)$$

The kinematic control law can be formulated by

$$\dot{\mathbf{h}}_d = \begin{bmatrix} v_c \\ \omega_c \end{bmatrix} = \begin{bmatrix} v_{l_ref} \cos e_{p3} + k_a e_{p1} \\ \omega_{ref} + v_{l_ref} (k_b e_{p2} + k_c \sin e_{p3}) \end{bmatrix} \quad (22)$$

where k_a, k_b, k_c are positive control coefficients. Using equation (22), one can rewrite equation (21) to form the kinematic closed-loop system as

$$\begin{aligned} \dot{\mathbf{e}}_p &= \begin{bmatrix} \dot{e}_{p1} \\ \dot{e}_{p2} \\ \dot{e}_{p3} \end{bmatrix} \\ &= \begin{bmatrix} -k_a e_{p1} + \omega_{ref} e_{p2} + v_{l_ref} (k_b e_{p2}^2 + k_c e_{p2} \sin e_{p3}) \\ -\omega_{ref} e_{p1} - v_{l_ref} (k_b e_{p1} e_{p2} + k_c e_{p1} \sin e_{p3}) + v_{l_ref} \sin e_{p3} \\ -v_{l_ref} (k_b e_{p2} + k_c \sin e_{p3}) \end{bmatrix} \end{aligned} \quad (23)$$

Now one can consider the following Lyapunov candidate as

$$V_k = \frac{1}{2} e_{p1}^2 + \frac{1}{2} e_{p2}^2 + \frac{1}{k_b} (1 - \cos e_{p3}) \quad (24)$$

Let us take the time derivative of (24) to obtain

$$\dot{V}_k = e_{p1} \dot{e}_{p1} + e_{p2} \dot{e}_{p2} + \frac{1}{k_b} \dot{e}_{p3} \sin e_{p3} \quad (25)$$

Applying (23) to (25) results in

$$\dot{V}_k = -k_a e_{p1}^2 - \frac{k_c}{k_b} \sin^2 e_{p3} \quad (26)$$

The equation (26) implies that e_{p1} and e_{p3} are asymptotically converged to zero and also by using LaSalle's principle, the convergence of e_{p2} to zero is ensured, as well (Kanayama et al., 1990).

3. Dynamic Controller Design

The designed kinematic controller in *Section 2* is very effective as long as there are no uncertainties. However, existing parametric/nonparametric uncertainties, and external disturbances which are unavoidable in the design of control structure, cause the implementation of kinematic controller trouble. To tackle this problem, a newly effective dynamic controller

goes along with the designed kinematic control law to ensure the accurate and desirable tracking performance.

The wheeled mobile robot's dynamics (Fukao et al., 2000; Haqshenas M. et al., 2020) in work-space considering permanent magnet DC motors can be formulated by

$$\mathbf{M}(\mathbf{q}) \frac{d^2 \mathbf{q}}{dt^2} + \mathbf{C} \left(\mathbf{q}, \frac{d\mathbf{q}}{dt} \right) \frac{d\mathbf{q}}{dt} + \mathbf{A}^T(\mathbf{q})\lambda + \mathbf{F} \left(\frac{d\mathbf{q}}{dt} \right) + \mathbf{G}(\mathbf{q}) + \boldsymbol{\tau}_d = \mathbf{B}(\mathbf{q})\boldsymbol{\tau}_R \quad (27)$$

$$\begin{aligned} \mathbf{J}_m \left(\mathbf{r}_g^{-1} \mathbf{J}^\dagger(\mathbf{q}) \frac{d^2 \mathbf{q}}{dt^2} + \mathbf{r}_g^{-1} \frac{d\mathbf{J}(\mathbf{q})^\dagger}{dt} \frac{d\mathbf{q}}{dt} \right) + \mathbf{B}_m \left(\mathbf{r}_g^{-1} \mathbf{J}^\dagger(\mathbf{q}) \frac{d\mathbf{q}}{dt} \right) + \mathbf{r}_g \boldsymbol{\tau}_R \\ = \mathbf{K}_m \mathbf{I}_m \end{aligned} \quad (28)$$

$$\mathbf{L}_m \frac{d\mathbf{I}_m}{dt} + \mathbf{R}_m \mathbf{I}_m + \mathbf{K}_b \left(\mathbf{r}_g^{-1} \mathbf{J}^\dagger(\mathbf{q}) \frac{d\mathbf{q}}{dt} \right) + \boldsymbol{\tau}_v = \mathbf{U} \quad (29)$$

where $\mathbf{M}(\mathbf{q}) \in \mathbb{R}^{3 \times 3}$ denotes the matrix of inertia, $\mathbf{C} \left(\mathbf{q}, \frac{d\mathbf{q}}{dt} \right) \frac{d\mathbf{q}}{dt} \in \mathbb{R}^{3 \times 1}$ represents the vector of Coriolis and centrifugal torques, $\mathbf{A}(\mathbf{q}) \in \mathbb{R}^{1 \times 3}$ is the holonomic constraint vector and $\lambda \in \mathbb{R}$ is the constraint force. Also, $\mathbf{F} \left(\frac{d\mathbf{q}}{dt} \right) \in \mathbb{R}^{3 \times 1}$, $\mathbf{G}(\mathbf{q}) \in \mathbb{R}^{3 \times 1}$ and $\boldsymbol{\tau}_d \in \mathbb{R}^{3 \times 1}$ denote friction, gravitational and disturbance vectors, respectively. The vector of robot torques is denoted by $\boldsymbol{\tau}_R \in \mathbb{R}^{2 \times 1}$ and $\mathbf{B}(\mathbf{q}) \in \mathbb{R}^{3 \times 2}$ is the transformation matrix to transform $\boldsymbol{\tau}_R$ from joint-space to work-space. In equation (28), $\mathbf{K}_m \in \mathbb{R}^{2 \times 2}$ is the torque constants, and $\mathbf{J}_m \in \mathbb{R}^{2 \times 2}$, $\mathbf{B}_m \in \mathbb{R}^{2 \times 2}$ and $\mathbf{r}_g \in \mathbb{R}^{2 \times 2}$ are the diagonal matrices of motors' inertia, damping and gear reduction ratio, respectively. Also, $\mathbf{J}^\dagger(\mathbf{q}) \in \mathbb{R}^{2 \times 3}$ represents the pseudoinverse of Jacobian matrix. In equation (29), $\mathbf{U} \in \mathbb{R}^{2 \times 1}$ is the vector of motors' voltages, $\boldsymbol{\tau}_v \in \mathbb{R}^{2 \times 1}$ is the external disturbances applied to the voltages, $\mathbf{L}_m \in \mathbb{R}^{2 \times 2}$, $\mathbf{R}_m \in \mathbb{R}^{2 \times 2}$ and $\mathbf{K}_b \in \mathbb{R}^{2 \times 2}$ are diagonal matrices of armatures' inductances, resistances, and back-emf constants, respectively. Let us write the time derivative of equation (8) as follows

$$\frac{d^2 \mathbf{q}}{dt^2} = \mathbf{S}(\theta) \frac{d^2 \mathbf{h}}{dt^2} + \left(\frac{d\mathbf{S}}{dt} \right) \left(\frac{d\mathbf{h}}{dt} \right) \quad (30)$$

By substituting equations (8) and (30) into equations (27-29), we have

$$\begin{aligned}
& \mathbf{B}^\dagger(\mathbf{q})\mathbf{M}(\mathbf{q})\mathbf{S}(\theta)\frac{d^2\mathbf{h}}{dt^2} + \mathbf{B}^\dagger(\mathbf{q})\left(\mathbf{M}(\mathbf{q})\frac{d\mathbf{S}}{dt} + \mathbf{C}(\mathbf{q}, \dot{\mathbf{q}})\mathbf{S}(\theta)\right)\frac{d\mathbf{h}}{dt} \\
& + \mathbf{B}^\dagger(\mathbf{q})\left(\mathbf{A}^T(\mathbf{q})\lambda + \mathbf{F}\left(\frac{d\mathbf{q}}{dt}\right) + \mathbf{G}(\mathbf{q}) + \boldsymbol{\tau}_d\right) = \boldsymbol{\tau}_R
\end{aligned} \tag{31}$$

$$\begin{aligned}
& J_m\mathbf{r}_g^{-1}\mathbf{J}^\dagger(\mathbf{q})\mathbf{S}(\theta)\frac{d^2\mathbf{h}}{dt^2} \\
& + \left(J_m\mathbf{r}_g^{-1}\frac{d\mathbf{J}(\mathbf{q})^\dagger}{dt}\mathbf{S}(\theta) + J_m\mathbf{r}_g^{-1}\mathbf{J}^\dagger(\mathbf{q})\frac{d\mathbf{S}}{dt} \right. \\
& \left. + \mathbf{B}_m\mathbf{r}_g^{-1}\mathbf{J}^\dagger(\mathbf{q})\mathbf{S}(\theta) \right)\frac{d\mathbf{h}}{dt} + \mathbf{r}_g\boldsymbol{\tau}_R = \mathbf{K}_m\mathbf{I}_m
\end{aligned} \tag{32}$$

$$\mathbf{L}_m\frac{d\mathbf{I}_m}{dt} + \mathbf{R}_m\mathbf{I}_m + \mathbf{K}_b\mathbf{r}_g^{-1}\mathbf{J}^\dagger(\mathbf{q})\mathbf{S}(\theta)\frac{d\mathbf{h}}{dt} + \boldsymbol{\tau}_v = \mathbf{U} \tag{33}$$

Now by applying equations (31) and (32) to (33), one can formulate the integrated dynamics of electrically-driven wheeled mobile robot as follows

$$\frac{d^2\mathbf{h}}{dt^2} + \mathbf{H} = \mathbf{U} \tag{34}$$

in which

$$\begin{aligned}
\mathbf{H} = & \left(\mathbf{R}_m \mathbf{K}_m^{-1} \left(\mathbf{J}_m \mathbf{r}_g^{-1} \frac{d\mathbf{J}(\mathbf{q})^\dagger}{dt} \mathbf{S}(\theta) + \mathbf{J}_m \mathbf{r}_g^{-1} \mathbf{J}^\dagger(\mathbf{q}) \frac{d\mathbf{S}}{dt} + \mathbf{B}_m \mathbf{r}_g^{-1} \mathbf{J}^\dagger(\mathbf{q}) \mathbf{S}(\theta) \right. \right. \\
& + \left. \left. \mathbf{r}_g \mathbf{B}^\dagger(\mathbf{q}) \left(\mathbf{M}(\mathbf{q}) \frac{d\mathbf{S}}{dt} + \mathbf{C} \left(\mathbf{q}, \frac{d\mathbf{q}}{dt} \right) \mathbf{S}(\theta) \right) \right) \right) \frac{d\mathbf{h}}{dt} \\
& + \left(\mathbf{K}_b \mathbf{r}_g^{-1} \mathbf{J}^\dagger(\mathbf{q}) \mathbf{S}(\theta) \right) \frac{d^2\mathbf{h}}{dt^2} \\
& + \left(\mathbf{R}_m \mathbf{K}_m^{-1} \left(\mathbf{J}_m \mathbf{r}_g^{-1} \mathbf{J}^\dagger(\mathbf{q}) \mathbf{S}(\theta) + \mathbf{r}_g \mathbf{B}^\dagger(\mathbf{q}) \mathbf{M}(\mathbf{q}) \mathbf{S}(\theta) \right) - \mathbf{I} \right) \frac{d^2\mathbf{h}}{dt^2} \\
& + \mathbf{R}_m \mathbf{K}_m^{-1} \mathbf{r}_g \mathbf{B}^\dagger(\mathbf{q}) \left(\mathbf{A}^T(\mathbf{q}) \boldsymbol{\lambda} + \mathbf{F} \left(\frac{d\mathbf{q}}{dt} \right) + \mathbf{G}(\mathbf{q}) + \boldsymbol{\tau}_d \right) + \mathbf{L}_m \dot{\mathbf{I}}_m \\
& + \boldsymbol{\tau}_v
\end{aligned} \tag{35}$$

where $\mathbf{I} \in \mathbb{R}^{3 \times 3}$ is the identity matrix. The great complexity of electrically-driven wheeled mobile robot's dynamics which express an uncertain multivariable system with highly coupled nonlinearity shown by equations (34-35) indicate a real challenge for control designers. Therefore, designing an efficient and powerful dynamic controller along with the kinematic controller (equation (22)) is unavoidable to tackle parametric and non-parametric uncertainties. Let us define the task-space tracking error, e_i , in a decentralized form as follows

$$e_i = h_{di} - h_i \tag{36}$$

where h_{di} is the desired task-space position and $i = \{1,2\}$. The objective of dynamic controller is to ensure the asymptotic convergence of e_i and \dot{e}_i to zero as well as the boundedness of all systems' signals. In order to design a state augmented adaptive backstepping control law, two variables namely, tracking error, e_i , and its time derivative, \dot{e}_i , along with an additional state as an integral of the tracking error, $\int_0^t e_i dt$, are considered as follows:

$$z_{1i} = \int_0^t e_i dt \tag{37}$$

$$\dot{z}_{1i} = z_{2i} = e_i \tag{38}$$

$$\dot{z}_{2i} = z_{3i} = \dot{e}_i = \dot{h}_{di} - \dot{h}_i \tag{39}$$

According to (39) and the decentralized form of (34), one can write \dot{z}_{3i} as follows

$$\dot{z}_{3i} = \ddot{e}_i = \ddot{h}_{di} - \dot{h}_i = \ddot{h}_{di} + H_i - U_i \quad (40)$$

This paper designs a Taylor series system to approximate H_i in the tracking error space as (Ahmadi and Fateh, 2018a; Ahmadi and Fateh, 2018b; Ahmadi and Fateh, 2019)

$$\begin{aligned} \hat{H}_i = & \sum_{p_1=0}^{m_1} \frac{\hat{H}_i^{(p_1)}(e_{i0})}{p_1!} \left(\int_0^\tau (e_i(\tau) - e_{i0}) d\tau \right)^{p_1} \\ & + \sum_{p_2=1}^{m_2} \frac{\hat{H}_i^{(p_2)}(e_{i0})}{p_2!} (e_i(t) - e_{i0})^{p_2} \\ & + \sum_{p_3=1}^{m_3} \frac{\hat{H}_i^{(p_3)}(\dot{e}_{i0})}{p_3!} (\dot{e}_i(t) - \dot{e}_{i0})^{p_3} \end{aligned} \quad (41)$$

where \hat{H}_i is the summation of m_1 -th and m_2 -th Taylor polynomials at the point of e_{i0} and m_3 -th Taylor polynomial at the point of \dot{e}_{i0} . One can represent equation (41) as

$$\hat{H}_i = \hat{\Theta}_i^T \mathbf{Y}_i \quad (42)$$

where $\hat{\Theta}_i^T \in \mathbb{R}^{1 \times (m_1+m_2+m_3+1)}$ is the vector of Taylor series parameters for \hat{H}_i , and $\mathbf{Y}_i \in \mathbb{R}^{(m_1+m_2+m_3+1) \times 1}$ is the vector of regressor given as

$$\begin{aligned} \mathbf{Y}_i = & \left[1, \left(\int_0^\tau (e_i(\tau) - e_{i0}) d\tau \right)^1, \dots, \left(\int_0^\tau (e_i(\tau) - e_{i0}) d\tau \right)^{m_1}, (e_i(t) \right. \\ & \left. - e_{i0})^1, \dots, (e_i(t) - e_{i0})^{m_2}, (\dot{e}_i(t) - \dot{e}_{i0})^1, \dots, (\dot{e}_i(t) \right. \\ & \left. - \dot{e}_{i0})^{m_3} \right]^T \end{aligned} \quad (43)$$

Let us model the uncertain nonlinear function H_i as follows

$$H_i = \Theta_i^T \mathbf{Y}_i + \varepsilon_i \quad (44)$$

in which ε_i is an approximation error and its upper bound can be introduced as

$$|\varepsilon_i| < \rho_i = \text{constant} \quad (45)$$

Considering (37-40) and (44), we rewrite the robotic system's dynamics as

$$\dot{z}_{1i} = z_{2i} \quad (46)$$

$$\dot{z}_{2i} = z_{3i} \quad (47)$$

$$\dot{z}_{3i} = \ddot{h}_{di} + \Theta_i^T Y_i + \varepsilon_i - U_i \quad (48)$$

Before developing a state augmented adaptive backstepping controller, some Assumptions are required to be considered:

Assumption 1. The desired task-space trajectory, \mathbf{h}_d , and its time derivatives, $\dot{\mathbf{h}}_d$ and $\ddot{\mathbf{h}}_d$ are all smooth and uniformly bounded.

Assumption 2. The external disturbances, $\boldsymbol{\tau}_d$ and $\boldsymbol{\tau}_v$ are bounded.

In order to design a robust controller recursively, one can decompose the system (46-48) into three subsystems. Considering the first subsystem as

$$\dot{z}_{1i} = z_{2i} \quad (49)$$

To stabilize the subsystem (49), A Lyapunov function can be given as

$$V_1 = \frac{1}{2} \sum_{i=1}^2 z_{1i}^2 \quad (50)$$

The derivative of (50) with respect to time yields

$$\dot{V}_1 = \sum_{i=1}^2 \dot{z}_{1i} z_{1i} = \sum_{i=1}^2 z_{2i} z_{1i} \quad (51)$$

By selecting the virtual controller z_{2i} as

$$z_{2i} = -k_{1i} z_{1i} \quad (52)$$

in which k_{1i} is a positive design parameter, the time derivative of Lyapunov function, \dot{V}_1 , can be given as

$$\dot{V}_1 = - \sum_{i=1}^2 k_{1i} z_{1i}^2 \quad (53)$$

Thus, the subsystem (49) is stabilized by choosing the virtual controller (52) since the equation (53) is negative semi-definite (i.e. $\dot{V}_1 \leq 0$). Now let us consider the second subsystem as follows

$$\dot{z}_{1i} = z_{2i} \quad (54)$$

$$\dot{z}_{2i} = z_{3i} \quad (55)$$

The Lyapunov function is chosen as follows

$$V_2 = V_1 + \frac{1}{2} \sum_{i=1}^2 (z_{2i} + k_{1i}z_{1i})^2 = \frac{1}{2} \sum_{i=1}^2 z_{1i}^2 + \frac{1}{2} \sum_{i=1}^2 (z_{2i} + k_{1i}z_{1i})^2 \quad (56)$$

The time derivative of (56) yields

$$\begin{aligned} \dot{V}_2 &= \sum_{i=1}^2 \dot{z}_{1i}z_{1i} + \sum_{i=1}^2 (z_{2i} + k_{1i}z_{1i})(\dot{z}_{2i} + k_{1i}\dot{z}_{1i}) \\ &= \sum_{i=1}^2 z_{2i}z_{1i} + \sum_{i=1}^2 (z_{2i} + k_{1i}z_{1i})(z_{3i} + k_{1i}z_{2i}) \end{aligned} \quad (57)$$

By selecting the virtual controller z_{3i} as

$$z_{3i} = -(k_{1i} + k_{2i})z_{2i} - (1 + k_{1i}k_{2i})z_{1i} + k_{1i}z_{2i} \quad (58)$$

Equation (57) can be formulated by

$$\begin{aligned} \dot{V}_2 &= \sum_{i=1}^2 z_{2i}z_{1i} + \sum_{i=1}^2 (z_{2i} + k_{1i}z_{1i})(-(k_{1i} + k_{2i})z_{2i} - (1 + k_{1i}k_{2i})z_{1i} + k_{1i}z_{2i}) \\ &= \sum_{i=1}^2 -k_{1i}z_{1i}^2 - k_{2i}(z_{2i} + k_{1i}z_{1i})^2 \leq 0 \end{aligned} \quad (59)$$

where $k_{2i} > 0$. Thus, the second subsystem, equations (54) and (55), is stabilized by choosing the virtual controller (58) since the equation (59) is negative semi-definite. Finally, the whole system (46-48) is considered and we choose the Lyapunov-like function V_3 as

$$\begin{aligned}
V_3 &= V_2 + \frac{1}{2} \sum_{i=1}^2 (z_{3i} + k_{1i}z_{2i} + z_{1i} + k_{2i}(z_{2i} + k_{1i}z_{1i}))^2 \\
&\quad + \sum_{i=1}^2 \frac{1}{2\gamma_i} (\boldsymbol{\Theta}_i - \widehat{\boldsymbol{\Theta}}_i)^T (\boldsymbol{\Theta}_i - \widehat{\boldsymbol{\Theta}}_i) \\
&= \frac{1}{2} \sum_{i=1}^2 z_{1i}^2 + \frac{1}{2} \sum_{i=1}^2 (z_{2i} + k_{1i}z_{1i})^2 \\
&\quad + \frac{1}{2} \sum_{i=1}^2 (z_{3i} + k_{1i}z_{2i} + z_{1i} + k_{2i}(z_{2i} + k_{1i}z_{1i}))^2 \\
&\quad + \sum_{i=1}^2 \frac{1}{2\gamma_i} (\boldsymbol{\Theta}_i - \widehat{\boldsymbol{\Theta}}_i)^T (\boldsymbol{\Theta}_i - \widehat{\boldsymbol{\Theta}}_i)
\end{aligned} \tag{60}$$

where γ_i is a positive constant. Taking the time derivative of V_3 gives that

$$\begin{aligned}
\dot{V}_3 &= \sum_{i=1}^2 z_{1i}\dot{z}_{1i} + \sum_{i=1}^2 (z_{2i} + k_{1i}z_{1i})(\dot{z}_{2i} + k_{1i}\dot{z}_{1i}) \\
&\quad + \sum_{i=1}^2 (z_{3i} + k_{1i}z_{2i} + z_{1i} + k_{2i}(z_{2i} + k_{1i}z_{1i}))(\dot{z}_{3i} + k_{1i}\dot{z}_{2i} \\
&\quad + \dot{z}_{1i} + k_{2i}(\dot{z}_{2i} + k_{1i}\dot{z}_{1i})) - \sum_{i=1}^2 \frac{1}{\gamma_i} (\boldsymbol{\Theta}_i - \widehat{\boldsymbol{\Theta}}_i)^T \dot{\boldsymbol{\Theta}}_i
\end{aligned} \tag{61}$$

By substituting (46-48) into (61) and using the upper bound of approximation error (45), we have

$$\begin{aligned}
\dot{V}_3 &\leq \sum_{i=1}^2 z_{1i}\dot{z}_{2i} + \sum_{i=1}^2 (z_{2i} + k_{1i}z_{1i})(z_{3i} + k_{1i}z_{2i}) \\
&\quad + \sum_{i=1}^2 (z_{3i} + k_{1i}z_{2i} + z_{1i} + k_{2i}(z_{2i} + k_{1i}z_{1i})) (\ddot{h}_{di} + \boldsymbol{\Theta}_i^T \mathbf{Y}_i + \rho_i \\
&\quad - U_i + k_{1i}z_{3i} + z_{2i} + k_{2i}(z_{3i} + k_{1i}z_{2i})) - \sum_{i=1}^2 \frac{1}{\gamma_i} (\boldsymbol{\Theta}_i - \widehat{\boldsymbol{\Theta}}_i)^T \dot{\boldsymbol{\Theta}}_i
\end{aligned} \tag{62}$$

This paper proposes the actual control law as

$$\begin{aligned}
U_i = & \ddot{h}_{di} + (1 + k_{1i}k_{2i})z_{2i} + (k_{1i} + k_{2i})z_{3i} + (z_{2i} + k_{1i}z_{1i}) \\
& + k_{3i}(z_{3i} + k_{1i}z_{2i} + z_{1i} + k_{2i}(z_{2i} + k_{1i}z_{1i})) + \hat{H}_i \\
& + \rho_i \text{sign}(z_{3i} + k_{1i}z_{2i} + z_{1i} + k_{2i}(z_{2i} + k_{1i}z_{1i}))
\end{aligned} \tag{63}$$

where k_{3i} is a positive constant, sign denotes the sign function and \hat{H}_i is calculated by equation (42), i.e. $\hat{H}_i = \hat{\Theta}_i^T \mathbf{Y}_i$. Applying the control law (63) to (62) results in

$$\begin{aligned}
\dot{V}_3 \leq & \sum_{i=1}^2 z_{1i}z_{2i} + \sum_{i=1}^2 (z_{2i} + k_{1i}z_{1i})(z_{3i} + k_{1i}z_{2i}) \\
& + \sum_{i=1}^2 (z_{3i} + k_{1i}z_{2i} + z_{1i} + k_{2i}(z_{2i} + k_{1i}z_{1i}))(\Theta_i - \hat{\Theta}_i)^T \mathbf{Y}_i \\
& - \sum_{i=1}^2 (z_{3i} + k_{1i}z_{2i} + z_{1i} + k_{2i}(z_{2i} + k_{1i}z_{1i})) \left(k_{1i}z_{3i} + z_{2i} \right. \\
& + k_{2i}(z_{3i} + k_{1i}z_{2i}) - (1 + k_{1i}k_{2i})z_{2i} - (k_{1i} + k_{2i})z_{3i} \\
& \left. - (z_{2i} + k_{1i}z_{1i}) - k_{3i}(z_{3i} + k_{1i}z_{2i} + z_{1i} + k_{2i}(z_{2i} + k_{1i}z_{1i})) \right) \\
& - \sum_{i=1}^2 \frac{1}{\gamma_i} (\Theta_i - \hat{\Theta}_i)^T \dot{\hat{\Theta}}_i
\end{aligned} \tag{64}$$

As a result, by selecting the adaptation rule as

$$\dot{\hat{\Theta}}_i = \gamma_i (z_{3i} + k_{1i}z_{2i} + z_{1i} + k_{2i}(z_{2i} + k_{1i}z_{1i})) \mathbf{Y}_i \tag{65}$$

And using some manipulations, one can rewrite equation (64) as follows

$$\begin{aligned}
\dot{V}_3 \leq & - \sum_{i=1}^2 k_{1i}z_{1i}^2 - \sum_{i=1}^2 k_{2i}(z_{2i} + k_{1i}z_{1i})^2 \\
& - \sum_{i=1}^2 k_{3i}(z_{3i} + k_{1i}z_{2i} + z_{1i} + k_{2i}(z_{2i} + k_{1i}z_{1i}))^2
\end{aligned} \tag{66}$$

Since k_{1i} , k_{2i} and k_{3i} are positive constants, equation (66) implies that the variables z_{2i} and z_{3i} (i.e. tracking error e_i and its time derivative \dot{e}_i) are converged to zero asymptotically. The boundedness of the desired path, h_{di} , and its time derivative, \dot{h}_{di} (*Assumption 1*), eventuate that h_i and \dot{h}_i are bounded. Moreover, the boundedness of $\Theta_i - \hat{\Theta}_i$ is assured via equation (60). Since γ_i , k_{1i} and k_{2i} are positive constants and the regressor matrix, \mathbf{Y}_i , is bounded via (43), the adaptation rule (65) shows that $\hat{\Theta}_i$ is bounded, as well. As a result, the boundedness of $\hat{\Theta}_i$

assures the boundedness of \hat{H}_i in (42). Then, the boundedness of control signal, U_i , is easily concluded via (63). Since $\mathbf{S}(\theta)$, which is the matrix of sinusoidal functions is bounded, the boundedness of $\dot{\mathbf{q}}$ is guaranteed via equation (8). Similarly, the matrices $\mathbf{J}(\mathbf{q})$, $\mathbf{J}^\dagger(\mathbf{q})$ and $\frac{d\mathbf{J}(\mathbf{q})^\dagger}{dt}$ are also bounded. The voltage equation (33) denotes a stable linear system and so the boundedness of U_i , $\boldsymbol{\tau}_v$ (Assumption 2), $\mathbf{J}^\dagger(\mathbf{q})$, $\dot{\mathbf{h}}$, $\mathbf{S}(\theta)$, \mathbf{r}_g and parameters of motors, including \mathbf{K}_b , \mathbf{R}_m and \mathbf{L}_m result in the boundedness of \mathbf{I}_m . The block diagram of control structure is shown in Figure. 3.

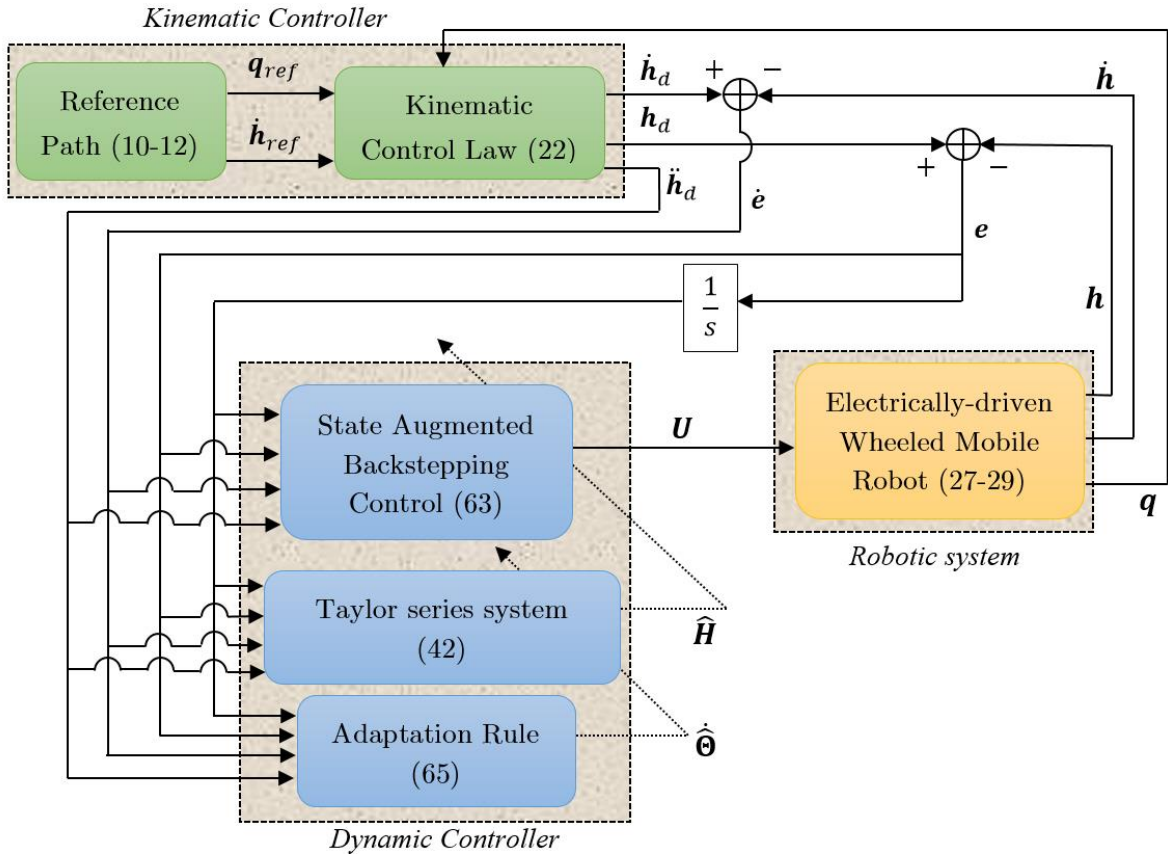


Figure. 3. The block diagram of proposed controller

4. Simulation Results

To demonstrate the usefulness of described control design, a desired circular path is produced via the reference linear velocity, $v_{l_ref} = 0.2$ m/sec, and the reference angular velocity, $\omega_{ref} = 0.1$ rad/sec. The initial posture for the WMR's reference path is chosen as $\mathbf{q}_{ref}(t_0 = 0) = [x_{ref}(0) \ y_{ref}(0) \ \theta_{ref}(0)]^T = [2 \ 0 \ \frac{\pi}{2}]^T$. Also, the initial posture of the real wheeled mobile robot is set to $\mathbf{q}(t_0 = 0) = [x(0) \ y(0) \ \theta(0)]^T = [-2 \ 5 \ \frac{7\pi}{4}]^T$. The dynamics of a wheeled mobile robot can be formulated by (Dong and Xu, 2001)

$$\mathbf{M}(\mathbf{q}) = \begin{bmatrix} m_w & 0 & -m_w d \sin(\theta) \\ 0 & m_w & m_w d \sin(\theta) \\ -m_w d \sin(\theta) & m_w d \sin(\theta) & I_w \end{bmatrix} \quad (67)$$

$$\mathbf{C}(\mathbf{q}, \dot{\mathbf{q}}) = \begin{bmatrix} 0 & 0 & -m_w d \dot{\theta} \cos(\theta) \\ 0 & 0 & m_w d \dot{\theta} \cos(\theta) \\ 0 & 0 & 0 \end{bmatrix} \quad (68)$$

$$\mathbf{G}(\mathbf{q}) = \mathbf{0} \quad (69)$$

$$\mathbf{F}(\dot{\mathbf{q}}) = 5\dot{\mathbf{q}} + 0.5\text{sgn}(\dot{\mathbf{q}}) \quad (70)$$

$$\mathbf{B}(\mathbf{q}) = \frac{1}{r_w} \begin{bmatrix} \cos(\theta) & \cos(\theta) \\ \sin(\theta) & \sin(\theta) \\ -b & b \end{bmatrix} \quad (71)$$

$$\mathbf{A}(\mathbf{q}) = [-\sin(\theta) \ \cos(\theta) \ 0] \quad (72)$$

$$\mathbf{J}(\mathbf{q}) = \frac{r_w}{2} \begin{bmatrix} \cos(\theta) & \cos(\theta) \\ \sin(\theta) & \sin(\theta) \\ \frac{1}{b} & -\frac{1}{b} \end{bmatrix} \quad (73)$$

in which m_w denotes the robot's mass and I_w is the mass moment of inertia. The numerical values for dynamical parameters of wheeled mobile robot and its DC permanent magnet motors are given in Table. 1 and Table. 2, respectively. To consider the dynamic external disturbances, let us formulate τ_{di} and τ_{vi} , as

$$\tau_{di} = a_{1i} + b_{1i} \sin(t) \quad (74)$$

$$\tau_{vi} = a_{2i} + b_{2i} \sin(t) \quad (75)$$

where (a_{1i}, b_{1i}) and (a_{2i}, b_{2i}) are chosen approximately one fourth of the maximum amplitude of robot's torque, τ_{Ri} , and motor's voltage, U_i , respectively. The parameters of kinematic controller (22), dynamic control law (63) and adaptation rule (65) are given in Table. 3. The reference and real paths in the XY plane are plotted in Figure. 4. Although the wheeled mobile robot starts moving relatively far from the initial posture of the reference path, the integrated kinematic/dynamic-based controller has successfully handled the problem of reference path tracking. In Figure. 5, the posture tracking error (17) is plotted to show the asymptotic convergence of \mathbf{q} to \mathbf{q}_{ref} . To confirm the efficiency of proposed dynamic control law (63), the asymptotic convergence of task-space tracking error, e_i , and its time derivative, \dot{e}_i , to zero are shown in Figures. 6(a) and 6(b), respectively. As illustrated in Figures. 6(a) and 6(b), signals e_i and \dot{e}_i contain small oscillations which are caused by the presence of dynamic external disturbances (74,75). The smooth and chattering-free control signals (63) are plotted in Figure. 7. It is noted that the relatively high values of control signals in the beginning are originated from the initial posture of the real wheeled mobile robot being relatively far from the reference path. For better evaluating, different initial conditions are also considered as follows

$$\mathbf{q}(t_0 = 0) = \left\{ \left[-3, -4, \frac{\pi}{4} \right]^T, \left[4, -3, \frac{\pi}{2} \right]^T, [5, 1, \pi]^T, \left[1, -1, \frac{\pi}{2} \right]^T, \left[4, 4, \frac{5\pi}{4} \right]^T, [-5, -1, 0]^T \right\} \quad (76)$$

All control parameters are chosen the same as Table. 3. The good tracking performance for all described initial situations (76), i.e. far and close initial conditions compared to the desired trajectory, without the need for readjusting the control parameters is shown in Figure. 8. Finally, the ‘‘Simscape Multibody’’ environment of ‘‘MATLAB’’ (Haqshenas M. et al., 2020) has been got to work to create the 3D design of wheeled mobile robot (Figure. 9) as well as to confirm the efficacy of obtained controller. The satisfactory tracking performance of control scheme is plotted in Figure. 10 utilizing four initial conditions.

As another means of evaluation, the proposed control law in this paper is compared with two well-designed controllers, namely an Adaptive Sliding Mode-based Disturbance Attenuation Control (ASMDAC) (Liu, K. et al., 2020) and an Adaptive Switching Gain-based Robust Control (ASGRC) (Roy, S. et al., 2017). Before introducing these comparative controllers, let us formulate the following performance indices via the kinematic and dynamic-based tracking errors:

$$\mathfrak{e}_1 = \frac{1}{T} \int_0^T (e_{p1}^2 + e_{p2}^2) dt \quad (77)$$

$$\mathbb{e}_2 = \frac{1}{T} \int_0^T e_{p3}^2 dt \quad (78)$$

$$\mathbb{e}_3 = \frac{1}{T} \int_0^T (e_1^2 + e_2^2) dt \quad (79)$$

$$\mathbb{e}_4 = \frac{1}{T} \int_0^T (\dot{e}_1^2 + \dot{e}_2^2) dt \quad (80)$$

where T is the time of simulation. In ASMDAC (Liu, K. et al., 2020) which has the integrated kinematic/dynamic-based control structure neglecting the actuators' dynamics, an adaptive sliding mode was utilized for the online estimation of lumped disturbance. Despite the presence of time-varying disturbance, ASMDAC achieves its control objectives without chattering phenomenon. The torque control input, $\boldsymbol{\tau}$, is designed as (Liu, K. et al., 2020)

$$\boldsymbol{\tau} = \mathbf{B}_0^{-1} \mathbf{M}_0 \left(\mathbf{M}_0^{-1} \mathbf{C}_0 \dot{\mathbf{h}} + \mathbf{e}_c(0) \exp(-\beta t) + \boldsymbol{\eta}_2 + \widehat{\mathbf{D}} + \text{sat}(\mathbf{s}) \right) \quad (81)$$

where $\mathbf{B}_0 \in \mathbb{R}^{2 \times 2}$, $\mathbf{M}_0 \in \mathbb{R}^{2 \times 2}$, and $\mathbf{C}_0 \in \mathbb{R}^{2 \times 2}$ are nominal values for the matrices of torque transformation, inertia, and Coriolis and centrifugal torques, respectively. Also, β is a positive scalar and $\widehat{\mathbf{D}} \in \mathbb{R}^{2 \times 1}$ and $\mathbf{s} \in \mathbb{R}^{2 \times 1}$ represent the adaptive sliding mode disturbance observer and the sliding surface, respectively. The kinematic controller, $\boldsymbol{\eta}_2 \in \mathbb{R}^{2 \times 1}$, is formulated by

$$\boldsymbol{\eta}_2 = \begin{bmatrix} v_r \cos e_{p3} + k_d \xi_1 \\ \omega_r + k_e v_r e_{p2} + k_f v_r \sin e_{p3} \end{bmatrix} \quad (82)$$

where

$$\dot{\xi}_1 = -Q \xi_1 + (P - \xi_1) \varpi^+(e_{p1}) - (N + \xi_1) \varpi^-(e_{p1}) \quad (83)$$

$$\varpi^+(e_{p1}) = \max(0, e_{p1}) \quad , \quad \varpi^-(e_{p1}) = \max(0, -e_{p1}) \quad (84)$$

in which P , N and Q are the rate of passive decay and k_d , k_e and k_f are positive design parameters. In equation (81), $\widehat{\mathbf{D}}$ and \mathbf{s} are formulated by

$$\dot{\widehat{\mathbf{D}}} = \mathbf{L} \widehat{\mathbf{D}} - \mathbf{L} (-\ddot{\mathbf{h}} - \mathbf{M}_0^{-1} \mathbf{C}_0 \dot{\mathbf{h}} + \mathbf{M}_0^{-1} \mathbf{B}_0 \boldsymbol{\tau}) \quad (85)$$

$$\mathbf{s} = \mathbf{e}_c(t) - \mathbf{e}_c(0) \exp(-\beta t) \quad (86)$$

where $\mathbf{L} = \text{diag}(l_1, l_2)$ is a negative definite symmetric matrix and $\mathbf{e}_c(t) \triangleq \boldsymbol{\eta}_2 - \dot{\mathbf{h}}$. According to equation (85), the feedbacks of acceleration are required (i.e. $\ddot{\mathbf{h}}$). Moreover, the term $\text{sat}(\mathbf{s})$ in equation (81) is given as

$$\text{sat}(\mathbf{s}) = \begin{cases} \hat{k} \frac{\mathbf{s}}{\|\mathbf{s}\|} & \text{if } \hat{k}\|\mathbf{s}\| \geq \zeta \\ \hat{k}^2 \frac{\mathbf{s}}{\zeta} & \text{if } \hat{k}\|\mathbf{s}\| < \zeta \end{cases} \quad (87)$$

where ζ is a small positive scalar and \hat{k} is the switching scalar formulated by the following adaptive rule

$$\dot{\hat{k}} = \gamma_1(\|\mathbf{s}\| - \gamma_2 \hat{k}) \quad (88)$$

where γ_1 and γ_2 are positive constants. The control parameters for ASMDAC is selected as Table. 4. Also, the simulation time, the desired trajectory, initial conditions, parameters of WMR, and external disturbances are chosen the same as our simulation results. The good tracking performance of ASMDAC and our proposed controller are illustrated in Figure. 11. Furthermore, the performance indices introduced in equations (77-80) for both controllers are given in Table. 5. Notice that the performance index, \mathfrak{e}_3 , is not calculated for ASMDAC since the feedbacks of e_1 and e_2 are not used in the control law (81).

Another comparison is provided with ASGRC (Roy, S. et al., 2017) which is a dynamic-based controller compensating for the un-modeled dynamics and modelling imperfection without considering the dynamic of actuators. The adaptive switching gain-based torque control signal, $\boldsymbol{\tau} \in \mathbb{R}^{2 \times 1}$, is developed as

$$\boldsymbol{\tau} = -\mathbf{e} - \mathbb{G}\mathbf{e}_f - \Delta\boldsymbol{\tau} \quad (89)$$

$$\Delta\boldsymbol{\tau} = \begin{cases} \hat{\rho} \frac{\mathbf{e}_f}{\|\mathbf{e}_f\|} & \text{if } \|\mathbf{e}_f\| \geq w \\ \hat{\rho} \frac{\mathbf{e}_f}{w} & \text{if } \|\mathbf{e}_f\| < w \end{cases} \quad (90)$$

where $\mathbb{G} \in \mathbb{R}^{2 \times 2}$ is a positive definite matrix, $w > 0$ is a small scalar, and $\mathbf{e}_f \triangleq \dot{\mathbf{e}} + \boldsymbol{\Omega}\mathbf{e} \in \mathbb{R}^{2 \times 1}$ is defined as the filtered tracking error (where $\boldsymbol{\Omega} \in \mathbb{R}^{2 \times 2}$ is a positive definite matrix). Also, $\hat{\rho}$ is formulated by

$$\hat{\rho} = \hat{\theta}_0 + \hat{\theta}_1 \|\boldsymbol{\zeta}\| + \hat{\theta}_2 \|\boldsymbol{\zeta}\|^2 + \gamma \quad (91)$$

where $\boldsymbol{\zeta} \triangleq [\mathbf{e} \quad \dot{\mathbf{e}}]^T \in \mathbb{R}^{4 \times 1}$ and $\hat{\theta}_j$ and γ are the adaptive auxiliary gain and the adaptive parameter, respectively formulated by ($j \in \{0,1,2\}$)

- For $\|\mathbf{e}_f\| \geq w$

$$\dot{\hat{\theta}}_j = \begin{cases} \alpha_j \|\boldsymbol{\zeta}\|^j \|\mathbf{e}_f\| & \{\mathbf{e}^T \dot{\mathbf{e}} > 0\} \cup \{\cup_{j=0}^2 \hat{\theta}_j \leq 0\} \cup \{\gamma \leq \beta\} \\ -\alpha_j \|\boldsymbol{\zeta}\|^j \|\mathbf{e}_f\| & \text{otherwise} \end{cases} \quad (92)$$

$$\dot{\gamma} = \begin{cases} \alpha_3 \|e_f\| & \{e^T \dot{e} > 0\} \cup \{\cup_{j=0}^2 \hat{\theta}_j \leq 0\} \cup \{\gamma \leq \beta\} \\ -\zeta \alpha_3 \|\zeta\|^4 & \text{otherwise} \end{cases}$$

- For $\|e_f\| < w$

$$\dot{\hat{\theta}}_i = 0, \dot{\gamma} = 0 \text{ with } \hat{\theta}_j(t_0) > 0, \gamma(t_0) > \beta \quad (93)$$

where $\alpha_0, \alpha_1, \alpha_2, \alpha_3, \beta, \zeta$ are positive scalars. Likewise, the simulation time, the desired trajectory, the parameters of WMR, and external disturbances are chosen the same as previous simulations. However, as discussed in Introduction, ASGRC has the challenging issue regarding initial conditions far from the desired trajectory since it is a dynamic-based controller. Thus, another initial condition is selected, $\mathbf{q}(t_0 = 0) = [1, -1, \frac{\pi}{2}]^T$, for evaluating the performance of both control laws. The control parameters of ASGRC are selected as Table. 6. In Figure. 12 and Table. 7, the tracking performance of ASGRC and our proposed controller are evaluated. According to Figure. 12 and Table. 7, for the initial condition near to the desired trajectory, ASGRC has a faster response yet higher tracking errors compared with our proposed controller. It is noted that in Table. 7, the performance indices, \mathfrak{e}_1 and \mathfrak{e}_2 are not calculated for ASGRC since a kinematic controller was not designed in its structure. The detailed comparisons among the proposed control and some relevant literature are also provided in Table. 8.

Table. 1. Dynamical Parameters of WMR.

b (m)	d (m)	I_w (Kg.m ²)	m_c (Kg)	r_w (m)
0.1	0.265	8	32	0.125

Table. 2. Dynamical and electrical parameters of DC Motors.

U_{max} (V)	R_m (Ω)	L_m (H)	K_b (V.s/rad)	K_m (N.m/A)	J_m (Nm.s ² /rad)	B_m (Nm.s/rad)	r_g
40	1.6	0.001	0.26	0.26	0.0002	0.001	0.05

Table. 3. Control parameters.

k_{1i}	k_{2i}	k_{3i}	γ_i	ρ_i	k_a	k_b	k_c
0.4	0.4	70	500	0.01	0.1	7	7

Table. 4. Control parameters of ASMDAC.

Q	P	N	β	ζ	l_1	l_2	γ_1	γ_2	k_d	k_e	k_f
0.5	1	1	9.5	0.0001	-20	-25	5	10	0.365	2.5	1.5

Table. 5. Comparison between ASMDAC and the proposed controller: The performance indices.

	e_1	e_2	e_3	e_4
The proposed controller	1.972	1.454	0.000025	0.00012
ASMDAC	1.991	1.557	-	0.00155

Table. 6. Control parameters of ASGRC.

α_i	α_3	ζ	w	β	\mathbb{G}	Ω
10	10	0.1	0.9	10	$\begin{bmatrix} 100 & 0 \\ 0 & 100 \end{bmatrix}$	$\begin{bmatrix} 0.8 & 0 \\ 0 & 0.8 \end{bmatrix}$

Table. 7. Comparison between ASGRC and the proposed controller: The performance indices

	e_1	e_2	e_3	e_4
The proposed controller	0.07944	0.02353	0.000023	0.00095
ASGRC	-	-	0.012754	0.00822

Table 8. Wheeled mobile robots: control structures.

Control methods	Case study	Motors' dynamics	Input (Torque/Voltage)	Controller type	Uncertainty	Far initial conditions	Stability type
Kanayama et al., (1990, May)	WMR	Neglected	Torque	Kinematic	-	Compensated	A ¹
JIANGdagger and Nijmeijer, 1997	WMR	Neglected	Torque	Kinematic	-	Compensated	UUB ²
Fierro and Lewis, 1997	WMR	Neglected	Torque	Kinematic /Dynamic	Parametric/non-parametric/dynamic disturbance	Compensated	A
Fukao et al., 2000	WMR	Neglected	Torque	Kinematic /Dynamic	Parametric	Compensated	A
De Luca et al., 2010	Wheeled Mobile Manipulator (WMM)	Neglected	Torque	Kinematic	-	Compensated	Not Checked
Shojaei et al., 2011	WMR	Considered	Voltage	Dynamic	Parametric/non-parametric/dynamic disturbance	Not Compensated	A
Rudra et al., 2016	WMR	Neglected	Torque	Dynamic	Parametric/non-parametric	Not Compensated	A
Roy, S. et al., 2017	WMR	Neglected	Torque	Dynamic	Parametric/non-parametric	Not Compensated	UUB
Souzanchi-K et al., 2017	WMM	Considered	Voltage	Dynamic	Parametric/non-parametric/dynamic disturbance	Not Compensated	BIBO ³
Nascimento et al., 2018	WMR	Neglected	Torque	Kinematic	-	Compensated	Not Checked
Wu et al., 2018	WMR	Neglected	Torque	Kinematic	-	Compensated	FT ⁴
Yang et al., 2018	WMR	Neglected	Torque	Kinematic /Dynamic	Parametric/non-parametric/dynamic disturbance	Compensated	A
Shu et al., 2018	WMR	Considered	Voltage	Kinematic /Dynamic	Parametric/non-parametric	Compensated	A
Huang et al., 2019	WMR	Neglected	Torque	Kinematic /Dynamic	Parametric/dynamic disturbance	Compensated	A
Zhai and Song, 2019	WMR	Neglected	Torque	Kinematic /Dynamic	Parametric/non-parametric/dynamic disturbance	Compensated	FT
Liu et al., 2020	WMR	Neglected	Torque	Kinematic /Dynamic	Parametric /dynamic disturbance	Compensated	FT
Haqshenas M. et al., 2020	WMR	Considered	Voltage	Dynamic	Parametric/non-parametric/dynamic disturbance	Not Compensated	A
The proposed controller	WMR	Considered	Voltage	Kinematic /Dynamic	Parametric/non-parametric/dynamic disturbance	Compensated	A

¹Asymptotic; ²Uniformly Ultimately Bounded; ³Boundary Input/Boundary Output; ⁴Finite time

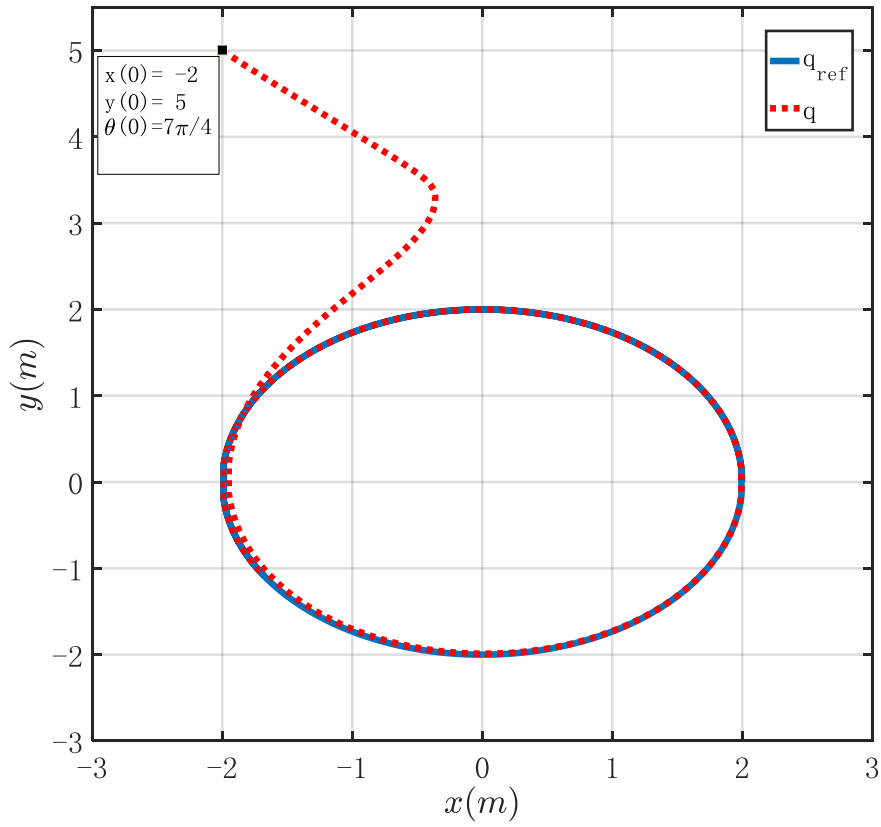


Figure 4. The proposed integrated kinematic/dynamic controller: Tracking performance.

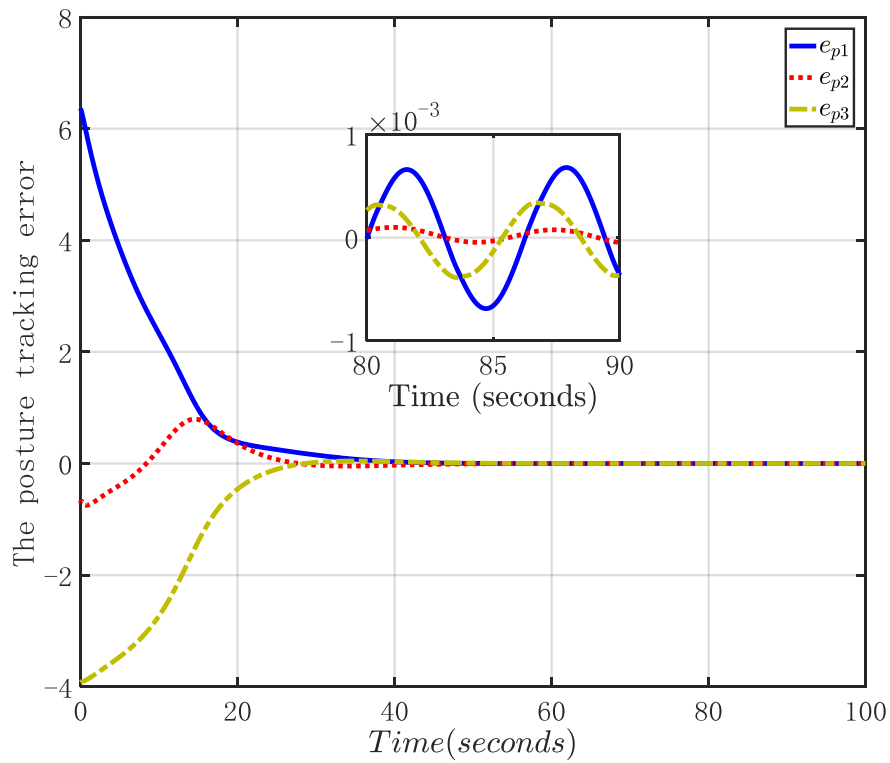


Figure 5. The proposed integrated kinematic/dynamic controller: The posture tracking error (17)

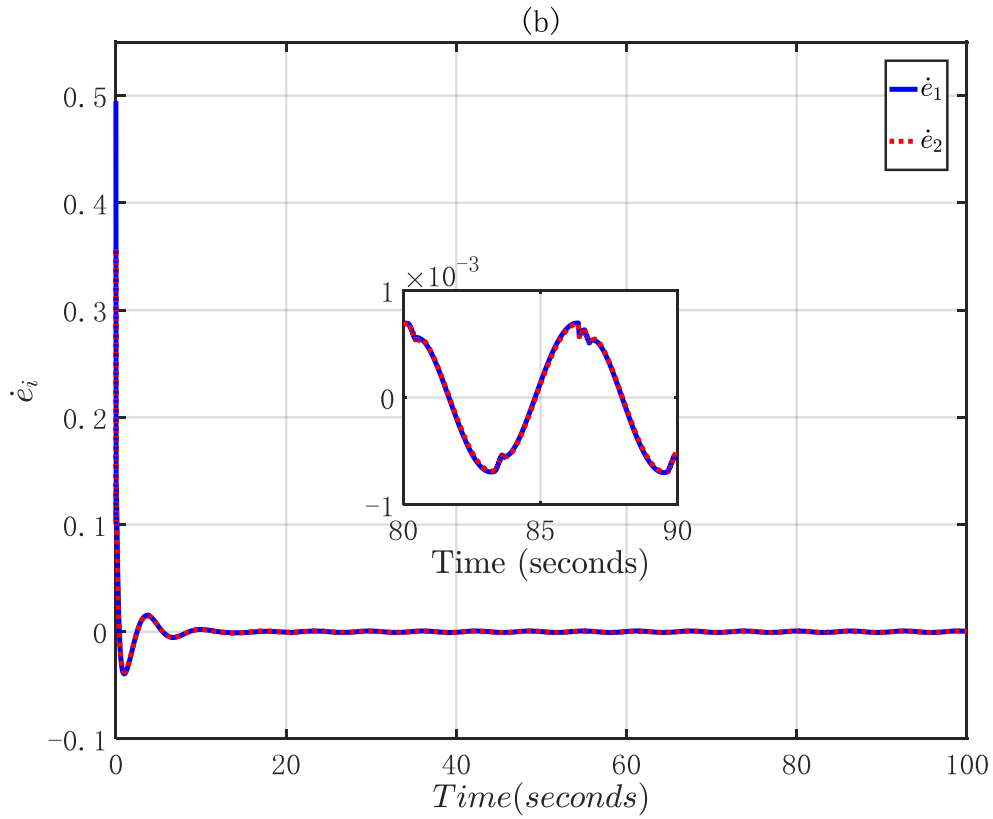
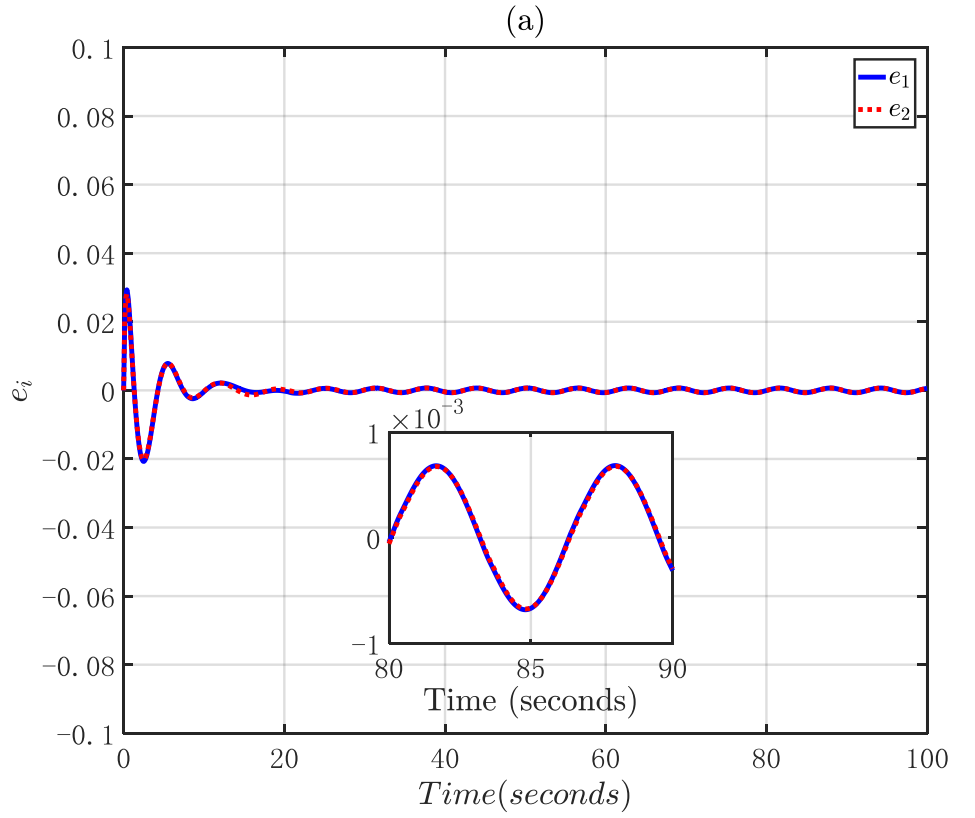


Figure 6. The proposed integrated kinematic/dynamic controller: (a) The task-space position tracking error (b) The task-space velocity tracking error

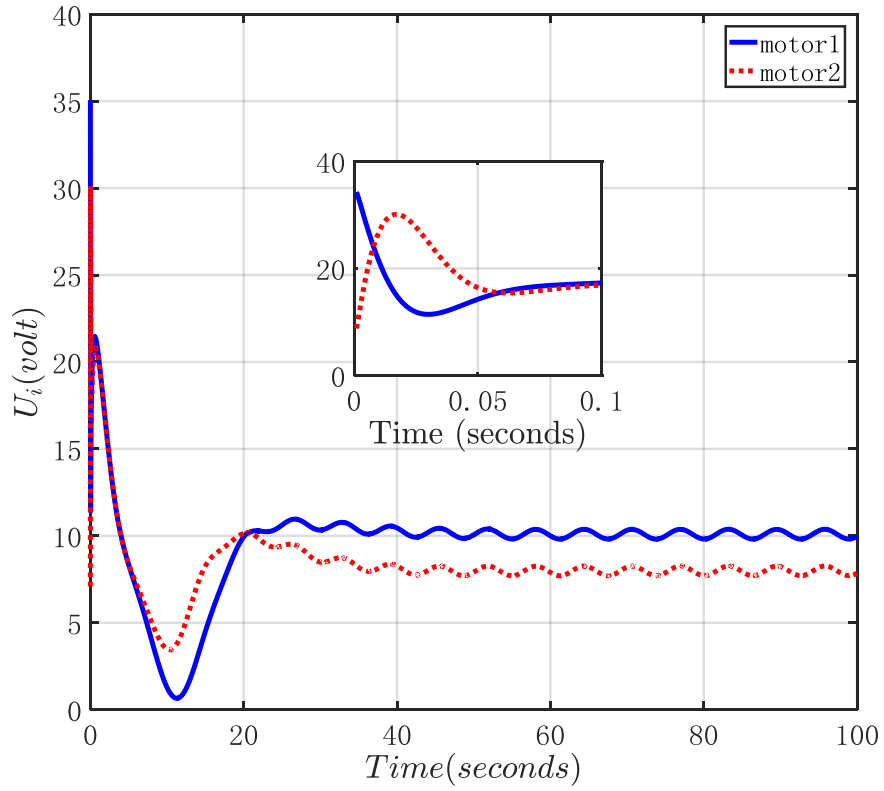


Figure. 7. The proposed integrated kinematic/dynamic controller: Control efforts (63)

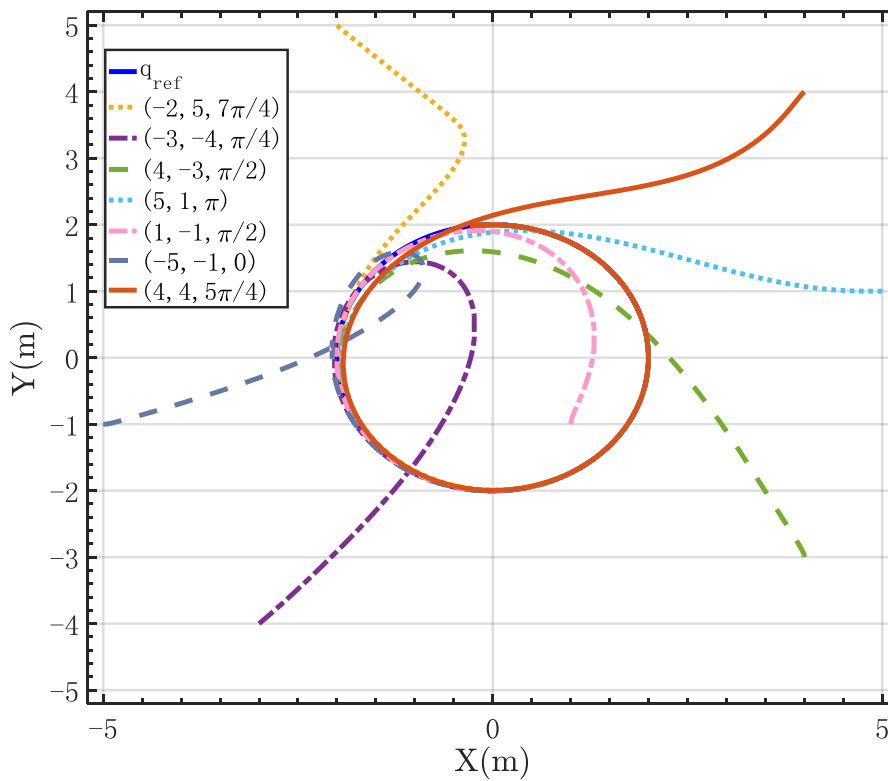


Figure. 8. The proposed integrated kinematic/dynamic controller: Tracking performance for difference initial conditions

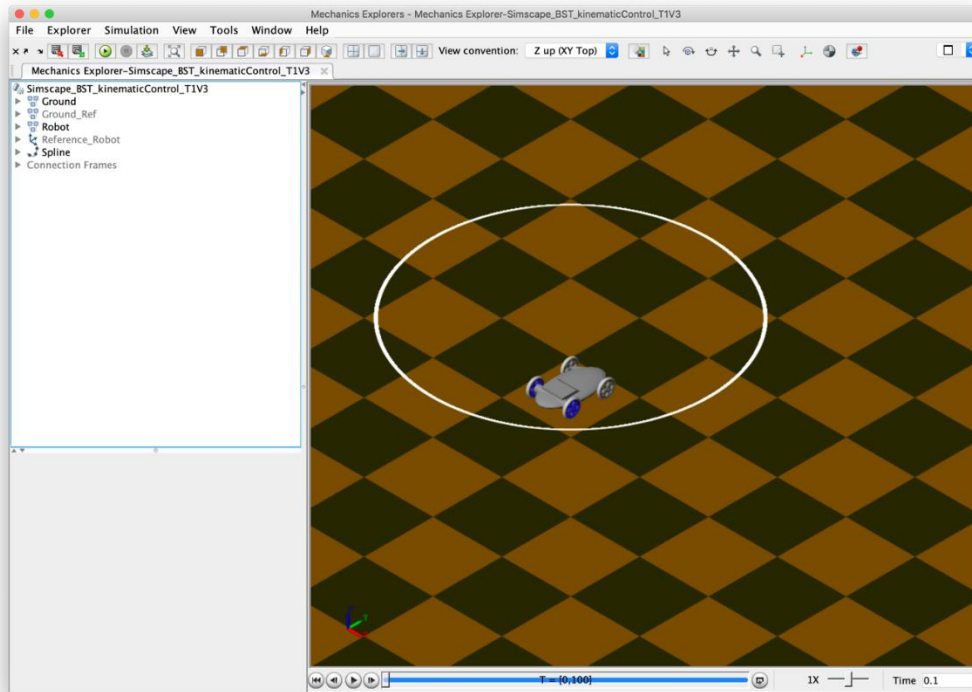


Figure. 9. The proposed integrated kinematic/dynamic controller: The WMR design utilizing “Simscape Multibody” environment.

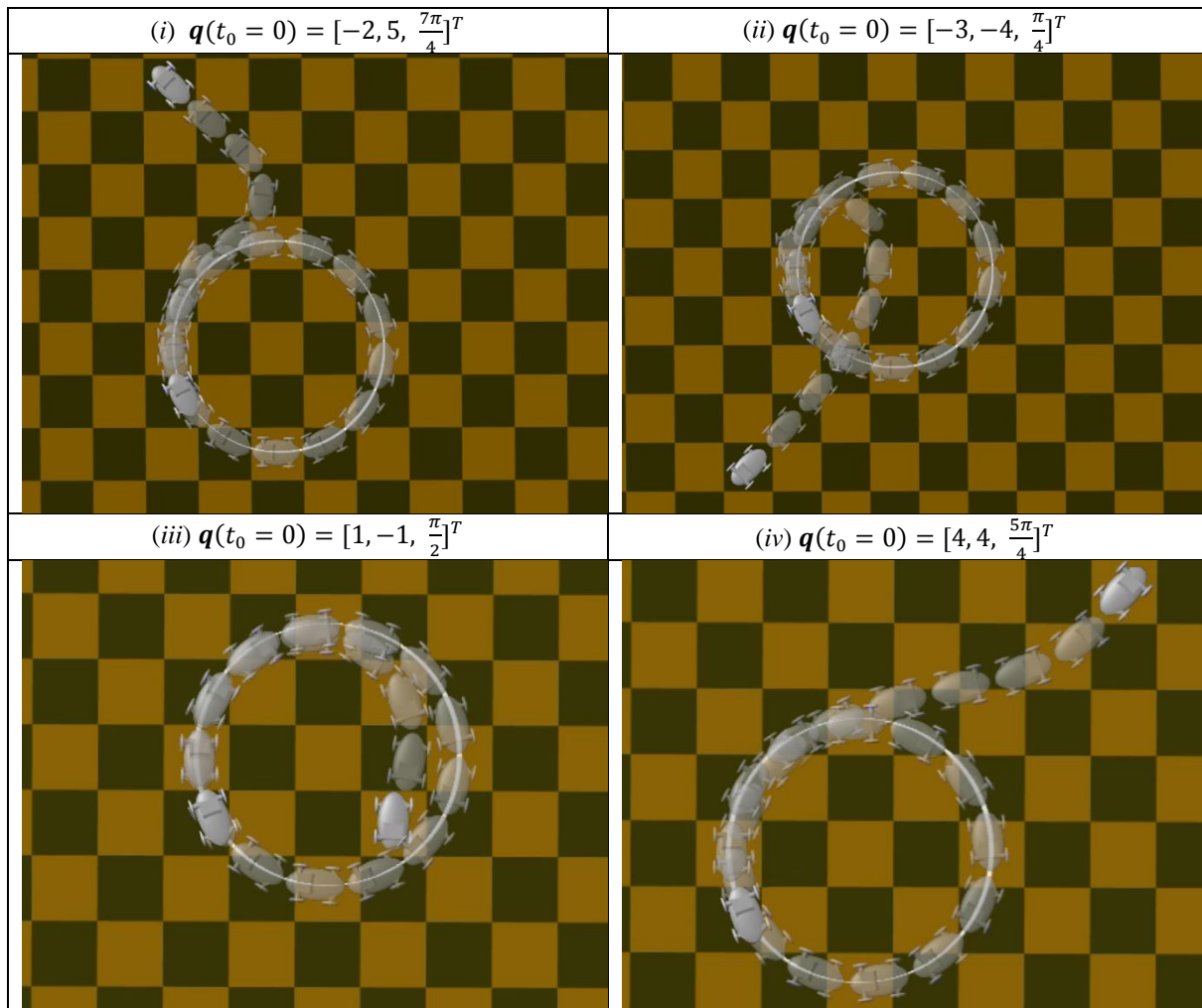


Figure. 10. The proposed integrated kinematic/dynamic controller: Tracking performance for circular desired path in “Simscape Multibody” environment.

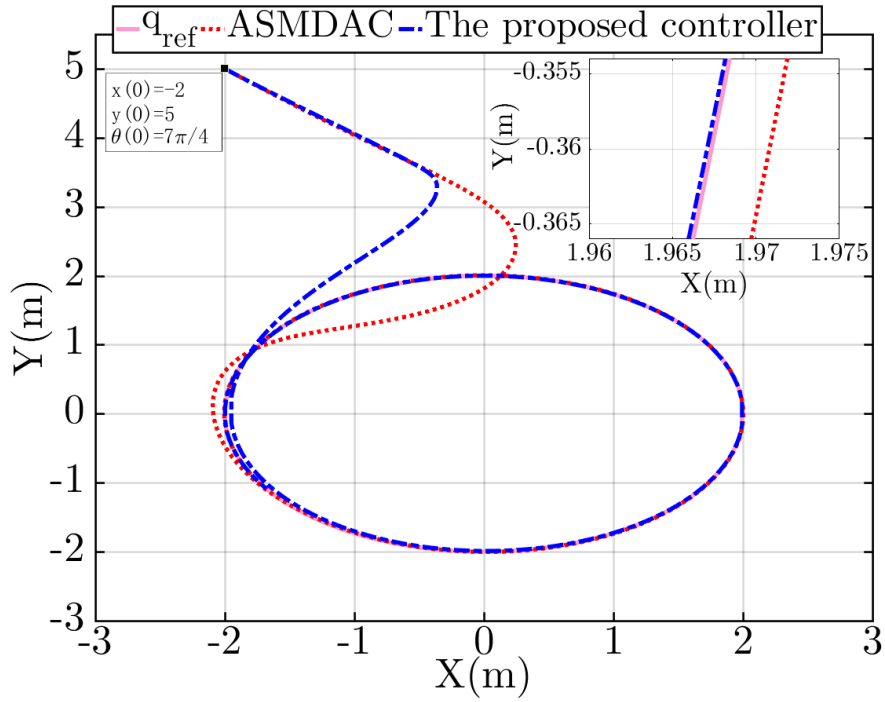


Figure. 11. The tracking performance of ASMDAC and proposed controller.

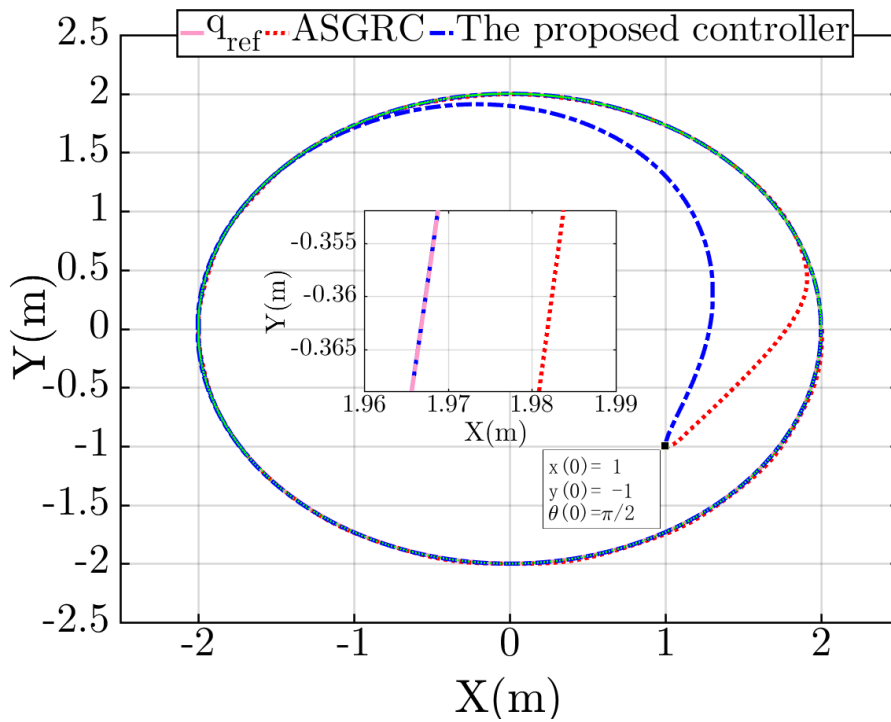


Figure. 12. The tracking performance of ASGRC and proposed controller.

5. Conclusion

This paper examines how to design a new integrated kinematic/dynamic tracking controller for electrically-driven wheeled mobile robots. The kinematic controller is utilized to minimize the posture tracking error as well as to generate a desired path for the dynamic control law. To solve the challenging issue regarding kinematic controllers raised by considering motors' dynamics and lumped uncertainties, including parametric, nonparametric and external disturbances, we propose the dynamic controller via a state augmented adaptive backstepping structure to track the desired path asymptotically in the face of lumped uncertainties. In the state augmented backstepping control, a new subsystem using an integral of the tracking error is added to obtain a precise tracking in comparison with the existing kinematic/dynamic controllers for wheeled mobile robots. Considering a circular desired path, the performance of the designed controller was evaluated based on several simulations, including relatively far initial postures of the real WMR in comparison with the reference path, 3D modeling and control of an electrically-driven WMR and also detailed comparisons with two recent well-designed controllers. The obtained results show the effectiveness of the designed control. For future directions, one can develop the proposed controller in this research by considering the effects of wheels' longitudinal and lateral slippage on the dynamics of electrically-driven WMRs and/or ensuring the finite time stability of closed-loop system.

References

- Aghababa, M. P., & Moradi, S. (2020). Robust adaptive dynamic surface back-stepping tracking control of high-order strict-feedback nonlinear systems via disturbance observer approach. *International Journal of Control*, doi: 10.1080/00207179.2020.1712478.
- Ahmadi, S. M., & Fateh, M. M. (2018a). Task-space asymptotic tracking control of robots using a direct adaptive Taylor series controller. *Journal of Vibration and Control*, 24(23), 5570-5584.
- Ahmadi, S. M., & Fateh, M. M. (2018b). Task-space control of robots using an adaptive Taylor series uncertainty estimator. *International Journal of Control*, doi: 10.1080/00207179.2018.1429673.
- Ahmadi, S. M., & Fateh, M. M. (2019). Composite direct adaptive Taylor series–fuzzy controller for the robust asymptotic tracking control of flexible-joint robots. *Transactions of the Institute of Measurement and Control*, doi: 10.1177/0142331219844806.
- Azimi, V., Nguyen, T. T., Sharifi, M., Fakoorian, S. A., & Simon, D. (2018). Robust ground reaction force estimation and control of lower-limb prostheses: Theory and simulation. *IEEE Transactions on Systems, Man, and Cybernetics: Systems*. doi: 10.1109/TSMC.2018.2836913
- Azimi, V., Shu, T., Zhao, H., Gehlhar, R., Simon, D., & Ames, A. D. (2019). Model-Based Adaptive Control of Transfemoral Prostheses: Theory, Simulation, and Experiments. *IEEE Transactions on Systems, Man, and Cybernetics: Systems*.
- Bayle, B., Fourquet, J. Y., Lamiroux, F., & Renaud, M. (2002, October). Kinematic control of wheeled mobile manipulators. In *IEEE/RSJ International Conference on Intelligent Robots and Systems* (Vol. 2, pp. 1572-1577). IEEE.
- Bu, X. (2018). Air-breathing hypersonic vehicles funnel control using neural approximation of non-affine dynamics. *IEEE/ASME Transactions On Mechatronics*, 23(5), 2099-2108.
- Bu, X., He, G., & Wang, K. (2018). Tracking control of air-breathing hypersonic vehicles with non-affine dynamics via improved neural back-stepping design. *ISA transactions*, 75, 88-100.
- Byrnes, C. I., & Isidori, A. (1989). New results and examples in nonlinear feedback stabilization. *Systems & Control Letters*, 12(5), 437-442.
- De Luca, A., Oriolo, G., & Giordano, P. R. (2010, May). Kinematic control of nonholonomic mobile manipulators in the presence of steering wheels. In *2010 IEEE International Conference on Robotics and Automation* (pp. 1792-1798). IEEE.
- De Luca, A., Oriolo, G., & Vendittelli, M. (2001). Control of wheeled mobile robots: An experimental overview. In *Ramsete* (pp. 181-226). Springer, Berlin, Heidelberg.
- Delgado-Mata, C., Velázquez, R., & Gutiérrez, C. A. (2012). A differential-drive mobile robot driven by an ethology inspired behaviour architecture. *Procedia Technology*, 3, 157-166.
- Dixon, W. E., Dawson, D. M., Zergeroglu, E., & Behal, A. (2001). Adaptive tracking control of a wheeled mobile robot via an uncalibrated camera system. *IEEE Transactions on Systems, Man, and Cybernetics, Part B (Cybernetics)*, 31(3), 341-352.
- Dong, Wenjie, and K-D. Kuhnert. "Robust adaptive control of nonholonomic mobile robot with parameter and nonparameter uncertainties." *IEEE Transactions on Robotics* 21.2 (2005): 261-266.
- Dong, W., & Xu, W. L. (2001). Adaptive tracking control of uncertain nonholonomic dynamic system. *IEEE Transactions on Automatic Control*, 46(3), 450-454.
- Fierro, R., & Lewis, F. L. (1997). Control of a nonholonomic mobile robot: Backstepping kinematics into dynamics. *Journal of robotic systems*, 14(3), 149-163.

- Fukao, T., Nakagawa, H., & Adachi, N. (2000). Adaptive tracking control of a nonholonomic mobile robot. *IEEE transactions on Robotics and Automation*, 16(5), 609-615.
- Haqshenas, M. A., Fateh, M. M., & Ahmadi, S. M. (2019, April). Indirect Adaptive Taylor Aeries Control of Differential Drive Wheeled Mobile Robots. In *2019 27th Iranian Conference on Electrical Engineering (ICEE)* (pp. 1040-1045). IEEE.
- Haqshenas M, A., Fateh, M. M., & Ahmadi, S. M. (2020). Adaptive control of electrically-driven nonholonomic wheeled mobile robots: Taylor series-based approach with guaranteed asymptotic stability. *International Journal of Adaptive Control and Signal Processing*. doi: 10.1002/acs.3104.
- Huang, J., Wen, C., Wang, W., & Jiang, Z. P. (2014). Adaptive output feedback tracking control of a nonholonomic mobile robot. *Automatica*, 50(3), 821-831.
- Huang, H., Zhou, J., Di, Q., Zhou, J., & Li, J. (2019). Robust neural network-based tracking control and stabilization of a wheeled mobile robot with input saturation. *International Journal of Robust and Nonlinear Control*, 29(2), 375-392.
- Ioannou, P. A., & Sun, J. (1996) *Robust Adaptive Control*. Englewood Cliffs, NJ: Prentice-Hall.
- JIANGdagger, Z. P., & Nijmeijer, H. (1997). Tracking control of mobile robots: a case study in backstepping. *Automatica*, 33(7), 1393-1399.
- Kanayama, Y., Kimura, Y., Miyazaki, F., & Noguchi, T. (1990, May). A stable tracking control method for an autonomous mobile robot. In *Proceedings., IEEE International Conference on Robotics and Automation* (pp. 384-389). IEEE.
- Kanayama, Y., Nilipour, A., & Lelm, C. A. (1988, April). A locomotion control method for autonomous vehicles. In *Proceedings. 1988 IEEE International Conference on Robotics and Automation* (pp. 1315-1317). IEEE.
- Khalil, H. K. (1992). *Nonlinear Systems*. Macmillan: New York.
- Klančar, G., Matko, D., & Blažič, S. (2009). Wheeled mobile robots control in a linear platoon. *Journal of Intelligent and Robotic Systems*, 54(5), 709-731.
- Klančar, G., Matko, D., & Blažič, S. (2011). A control strategy for platoons of differential drive wheeled mobile robot. *Robotics and Autonomous Systems*, 59(2), 57-64.
- Klancar, G., Zdesar, A., Blazic, S., & Skrjanc, I. (2017). *Wheeled mobile robotics: from fundamentals towards autonomous systems*. Butterworth-Heinemann.
- Kokotovic, P. V. (1992). The joy of feedback: nonlinear and adaptive. *IEEE Control Systems Magazine*, 12(3), 7-17.
- Krstic, M., Kokotovic, P. V., & Kanellakopoulos, I. (1995). *Nonlinear and adaptive control design*. John Wiley & Sons, Inc.
- Lee, J. H., Lin, C., Lim, H., & Lee, J. M. (2009). Sliding mode control for trajectory tracking of mobile robot in the RFID sensor space. *International Journal of Control, Automation and Systems*, 7(3), 429-435.
- Le-Tien, L., & Albu-Schäffer, A. (2017). Robust adaptive tracking control based on state feedback controller with integrator terms for elastic joint robots with uncertain parameters. *IEEE Transactions on Control Systems Technology*, 26(6), 2259-2267.
- Liu, K., Gao, H., Ji, H., & Hao, Z. (2020). Adaptive Sliding Mode Based Disturbance Attenuation Tracking Control for Wheeled Mobile Robots. *International Journal of Control, Automation and Systems*, doi: 10.1007/s12555-019-0262-7.

- Luo, S., Wu, S., Liu, Z., & Guan, H. (2014). Wheeled mobile robot RBFNN dynamic surface control based on disturbance observer. *ISRN Applied Mathematics*, 2014.
- Mirzaeinejad, H., & Shafei, A. M. (2018). Modeling and trajectory tracking control of a two-wheeled mobile robot: Gibbs–Appell and prediction-based approaches. *Robotica*, 36(10), 1551-1570.
- Nascimento, T. P., Dórea, C. E. T., & Gonçalves, L. M. G. (2018). Nonlinear model predictive control for trajectory tracking of nonholonomic mobile robots: A modified approach. *International Journal of Advanced Robotic Systems*, 15(1), doi: 10.1177/1729881418760461.
- Park, B. S., Yoo, S. J., Park, J. B., & Choi, Y. H. (2009). A simple adaptive control approach for trajectory tracking of electrically driven nonholonomic mobile robots. *IEEE Transactions on Control Systems Technology*, 18(5), 1199-1206.
- Roy, S., Roy, S. B., & Kar, I. N. (2017). Adaptive–robust control of Euler–Lagrange systems with linearly parametrizable uncertainty bound. *IEEE Transactions on Control Systems Technology*, 26(5), 1842-1850.
- Rudra, S., Barai, R. K., & Maitra, M. (2016). Design and implementation of a block-backstepping based tracking control for nonholonomic wheeled mobile robot. *International Journal of Robust and Nonlinear Control*, 26(14), 3018-3035.
- Saberi, A., Kokotovic, P. V., & Sussmann, H. J. (1990). Global stabilization of partially linear composite systems. *SIAM Journal on Control and Optimization*, 28(6), 1491-1503.
- Škrjanc, I., & Klančar, G. (2017). A comparison of continuous and discrete tracking-error model-based predictive control for mobile robots. *Robotics and autonomous systems*, 87, 177-187.
- Shaocheng, T., Changying, L., & Yongming, L. (2009). Fuzzy adaptive observer backstepping control for MIMO nonlinear systems. *Fuzzy sets and systems*, 160(19), 2755-2775.
- Shu, P., Oya, M., & Zhao, J. (2018). A new adaptive tracking control scheme of wheeled mobile robot without longitudinal velocity measurement. *International Journal of Robust and Nonlinear Control*, 28(5), 1789-1807.
- Shojaei, K., Shahri, A. M., & Tarakameh, A. (2011). Adaptive feedback linearizing control of nonholonomic wheeled mobile robots in presence of parametric and nonparametric uncertainties. *Robotics and Computer-Integrated Manufacturing*, 27(1), 194-204.
- Slotine, J. J., & Coetsee, J. A. (1986). Adaptive sliding controller synthesis for non-linear systems. *International Journal of Control*, 43(6), 1631-1651.
- Slotine, J. J. E., & Li, W. (1991). *Applied nonlinear control* (Vol. 199, No. 1). Englewood Cliffs, NJ: Prentice hall.
- Slotine, J. J., & Weiping, L. (1988). Adaptive manipulator control: A case study. *IEEE transactions on automatic control*, 33(11), 995-1003.
- Souzanchi-K, M., Arab, A., Akbarzadeh-T, M. R., & Fateh, M. M. (2017). Robust impedance control of uncertain mobile manipulators using time-delay compensation. *IEEE Transactions on Control Systems Technology*, 26(6), 1942-1953.
- Spooner, J. T., Maggiore, M., Ordonez, R., & Passino, K. M. (2004). *Stable adaptive control and estimation for nonlinear systems: neural and fuzzy approximator techniques* (Vol. 43). John Wiley & Sons.
- Swaroop, D. V. A. H. G., Gerdes, J. C., Yip, P. P., & Hedrick, J. K. (1997, June). Dynamic surface control of nonlinear systems. In *Proceedings of the 1997 American Control Conference (Cat. No. 97CH36041)* (Vol. 5, pp. 3028-3034). IEEE.
- Tsinias, J. (1989). Sufficient Lyapunov-like conditions for stabilization. *Mathematics of control, Signals and Systems*, 2(4), 343-357.

- Van, M., Mavrovouniotis, M., & Ge, S. S. (2018). An adaptive backstepping nonsingular fast terminal sliding mode control for robust fault tolerant control of robot manipulators. *IEEE Transactions on Systems, Man, and Cybernetics: Systems*, 49(7), 1448-1458.
- Wang, C. H., Liu, H. L., & Lin, T. C. (2002). Direct adaptive fuzzy-neural control with state observer and supervisory controller for unknown nonlinear dynamical systems. *IEEE Transactions on Fuzzy Systems*, 10(1), 39-49.
- Wu, D., Cheng, Y., Du, H., Zhu, W., & Zhu, M. (2018). Finite-time output feedback tracking control for a nonholonomic wheeled mobile robot. *Aerospace Science and Technology*, 78, 574-579.
- Wu, X., Jin, P., Zou, T., Qi, Z., Xiao, H., & Lou, P. (2019). Backstepping trajectory tracking based on fuzzy sliding mode control for differential mobile robots. *Journal of Intelligent & Robotic Systems*, 96(1), 109-121.
- Xin, L. P., Yu, B., Zhao, L., & Yu, J. (2020). Adaptive fuzzy backstepping control for a two continuous stirred tank reactors process based on dynamic surface control approach. *Applied Mathematics and Computation*, doi: 10.1016/j.amc.2020.125138.
- Yang, J. M., & Kim, J. H. (1999). Sliding mode control for trajectory tracking of nonholonomic wheeled mobile robots. *IEEE Transactions on robotics and automation*, 15(3), 578-587.
- Yang, F., Su, H., Wang, C., & Li, Z. (2018). Adaptive and sliding mode tracking control for wheeled mobile robots with unknown visual parameters. *Transactions of the Institute of Measurement and Control*, 40(1), 269-278.
- Yip, P. P., & Hedrick, J. K. (1998). Adaptive dynamic surface control: a simplified algorithm for adaptive backstepping control of nonlinear systems. *International Journal of Control*, 71(5), 959-979.
- Yoo, S. J., Park, J. B., & Choi, Y. H. (2005, June). Direct adaptive control using self recurrent wavelet neural network via adaptive learning rates for stable path tracking of mobile robots. In *Proceedings of the 2005, American Control Conference, 2005*. (pp. 288-293). IEEE.
- Yue, M., Zhang, Y., & Tang, F. (2013). Path following control of a two-wheeled surveillance vehicle based on sliding mode technology. *Transactions of the Institute of Measurement and Control*, 35(2), 212-218.
- Yoo, S. J., Park, J. B., & Choi, Y. H. (2010). Adaptive formation tracking control of electrically driven multiple mobile robots. *IET control theory & applications*, 4(8), 1489-1500.
- Zhai, J. Y., & Song, Z. B. (2019). Adaptive sliding mode trajectory tracking control for wheeled mobile robots. *International Journal of Control*, 92(10), 2255-2262.
- Zhang, Y., Wen, C., & Soh, Y. C. (2000). Adaptive backstepping control design for systems with unknown high-frequency gain. *IEEE Transactions on Automatic Control*, 45(12), 2350-2354.